ARKIV FÖR FYSIK

UTGIVET AV

KUNGL. SVENSKA VETENSKAPSAKADEMIEN

Band 9 nr 32

OLOF BECKMAN

Relative intensities of the X-ray *K* lines of heavier elements

---

STOCKHOLM

ALMQVIST & WIKSELLS BOKTRYCKERI AB

LONDON

H. K. LEWIS & CO., LTD

136, GOWER STREET

1955

PARIS

LIBRAIRIE C. KLINCKSIECK

11 RUE DE LILLE

Digitized by the Internet Archive
in 2026

https://archive.org/details/IA41548912_0001

RELATIVE INTENSITIES OF THE X-RAY *K* LINES OF HEAVIER ELEMENTS

INAUGURAL DISSERTATION

BY

OLOF BECKMAN

FIL. LIC., ÖSTG.

BY DUE PERMISSION OF THE PHILOSOPHICAL FACULTY
OF THE UNIVERSITY OF UPPSALA, TO BE PUBLICLY DISCUSSED
IN THE LECTURE HALL OF THE INSTITUTE OF PHYSICS,
ON MAY 24TH, 1955, AT 10 A.M., FOR THE DEGREE
OF DOCTOR OF PHILOSOPHY

UPPSALA 1955

ALMQVIST & WIKSELLS BOKTRYCKERI AB

P. UNIV.
BIBLIOTHEEK
LEIDEN.

ARKIV FÖR FYSIK Band 9 nr 32

Communicated 23 February 1955 by MANNE SIEGBAHN and GUNNAR HÄGG

Relative intensities of the X-ray *K* lines of heavier elements

By OLOF BECKMAN

With 19 figures in the text

Contents

Acknowledgements 495
Chapter I. Introduction 496
Chapter II. Experimental arrangements 497
1. The van de Graaff generator 497
2. The voltmeter 499
3. Target arrangements 499
4. The current integrator 501
5. The spectrometer 502
6. The scintillation counter 505
7. Shielding 505
Chapter III. Recordings with the spectrometer 506
1. Adjustment 506
2. Procedure 507
Chapter IV. Computation of the X-ray intensities 507
1. The efficiency of the scintillation counter 513
2. Absorption of the X-ray beam 514
3. X-ray absorption in the target 514
4. Reflection properties of the quartz crystal 516
Chapter V. Discussion of the results 519
1. General remarks on *K*-spectra 519
2. Earlier investigations 520
3. The present measurements 521
Chapter VI. The KL_1-transition 526

Acknowledgements

The investigation reported in this paper was carried out at the Physical Laboratory of Uppsala University. I am greatly indebted to Professor AXEL E. LINDH, formerly head of the Physical Laboratory, for the kind interest and constant encouragement he has provided throughout my work.

I wish to express my sincere gratitude to Professor PER OHLIN, who made the first designs of the van de Graaff machine essential to this work, for the valuable help he has offered me during this investigation.

My sincere thanks are also due to Professor KAI SIEGBAHN, Laborator ARNE SANDSTRÖM and Docent GÖSTA BROGREN, who have given freely of their time in discussions of problems that have arisen.

The experimental measurements in the concluding part of the study were assisted to a large extent and in a very skilful manner by Fil. kand. PÄR BERGWALL.

Finally my thanks are due to Professor HARRISON SHULL for correcting my English.

Uppsala, March, 1955.

CHAPTER I

Introduction

In spite of the great number of investigations on X-ray spectra only a few measurements have been made of the intensities of the lines. Intensity measurements are most easily carried out in the case of K-spectra, where all lines are excited at the same voltage and consequently the intensity ratios are independent of the mode of excitation. Investigations of the K line intensities of elements in the middle of the periodic system have been made by MEYER [1929] ($Z = 23$–49) and by WILLIAMS [1933] ($Z = 24$–52). KLIEVER [1939] has measured the intensities of the K lines of tungsten and platinum by means of an X-ray spectrometer and an ionization chamber. A method with different absorption filters has been applied by VOTH [1942] in an investigation of several heavy elements.

Theoretical calculations in this field have been made by PINCHERLE [1933] and by MASSEY and BURHOP [1936], but their results are not satisfactorily checked by the rather few results that have been obtained experimentally. Thus it was of great interest to measure the K line intensities of as many of the heavier elements as might be available and to study the change in the line intensities with the atomic number, Z.

Such an investigation could conveniently be carried out with the van de Graaff generator of the Physical Laboratory. A high luminosity spectrometer with a counter of high efficiency would probably give enough intensity for registering even the weaker lines of the K-spectrum.

X-ray intensity measurements employing pulse-counting devices require constant conditions for long periods of time. One possible way of meeting these conditions is to stabilize both voltage and current in the X-ray tube and to count the X-ray quanta entering the counting tube for a known time. It is very difficult, however, to stabilize satisfactorily the tube current of van de Graaff generators, and thus it would be better to use some type of monitor method. In the present experiments it seemed most suitable to use the electron beam as a monitor. The target is insulated from the earth and connected to a current integrator. The counter that registers the X-rays is switched on for the same period of time in which the current integrator records the charge reaching the target. Since the X-ray yield in the target varies very rapidly with the energy of the electrons, the high voltage must be well stabilized. Furthermore it is necessary to keep the focal spot in a fixed position on the target.

It is essential to have an X-ray spectrometer of high luminosity and high dispersion. These demands are met by the curved crystal spectrograph and, for the short wavelengths in question (100–220 XU), the transmission type is the only one available.

In this spectrometer the radiation from an extended focal spot (Fig. 1) is reflected at the inner atomic planes in the crystal and focussed to a point on the Rowland circle. Radiation from different points of the focal spot is reflected by different parts of the crystal; thus the focal spot corresponds to a "reflecting area" of the crystal. If the crystal aperture is large enough, radiation from the whole focal spot is utilized. On the other hand, if the crystal opening is too small, the whole crystal aperture is filled with radiation, but only a part of the focal spot is used. In the latter case, fluc-

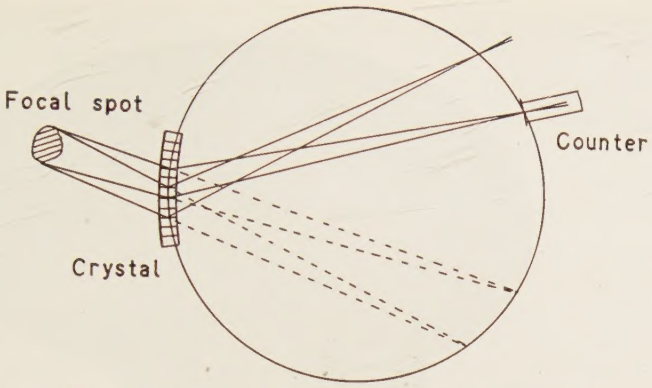

Fig. 1. Principle of the curved crystal spectrometer.

tuations in the intensity distribution from the focal spot may cause changes in the intensity of the X-rays reflected by the crystal, even though the electron beam current is constant. This may introduce severe errors when the electron beam itself is used as a monitor. Thus there must not be any limiting aperture or slit between the X-ray tube and the counter-slit.

As shown in Fig. 1, the crystal is mounted in a fixed position, limiting the spectrograph to only a rather narrow wavelength region. Different wavelengths are reflected from different parts of the crystal, and it is difficult to ascertain the wavelength at which the crystal holder starts to screen the X-ray beam.

The spectrometer should be constructed preferably in such a manner that the crystal is moved simultaneously with, and at half the angular speed of the counter-slit. Moreover, the crystal opening must be broader than the width of the focal spot. By this arrangement always the same (central) part of the crystal is used for X-ray reflection. In order to minimize the broadening of the lines the vertical height of the X-ray beam must be low. This is accomplished by making the angle between the target and the plane of the Rowland circle rather small.

Because of their good elastic qualities, quartz crystals are very useful in curved crystal spectrographs. The short wavelengths make it necessary to use a crystal plane with a low grating constant, but at the same time the plane must, of course, have good reflecting properties. Suitable planes are, for instance, quartz $13\bar{4}0$, $22\bar{4}3$ and $50\bar{5}2$. For the present spectrograph, $22\bar{4}3$ was chosen. This plane has a grating constant of 1012.75 XU and a crystal structure factor of 15.6. The wavelength region 100–220 XU then corresponds to the Bragg angles 2°.9–6°.2. In the case of tungsten some measurements were also made employing the plane $13\bar{4}0$ with the grating constant 1177.63 XU and structure factor 20.9.

Chapter II

Experimental arrangements

1. The van de Graaff generator

The van de Graaff generator (Fig. 2) is an open-air machine with two charging belts driven by three-phase asynchronous motors. The velocity of the belts is 20 m/sec,

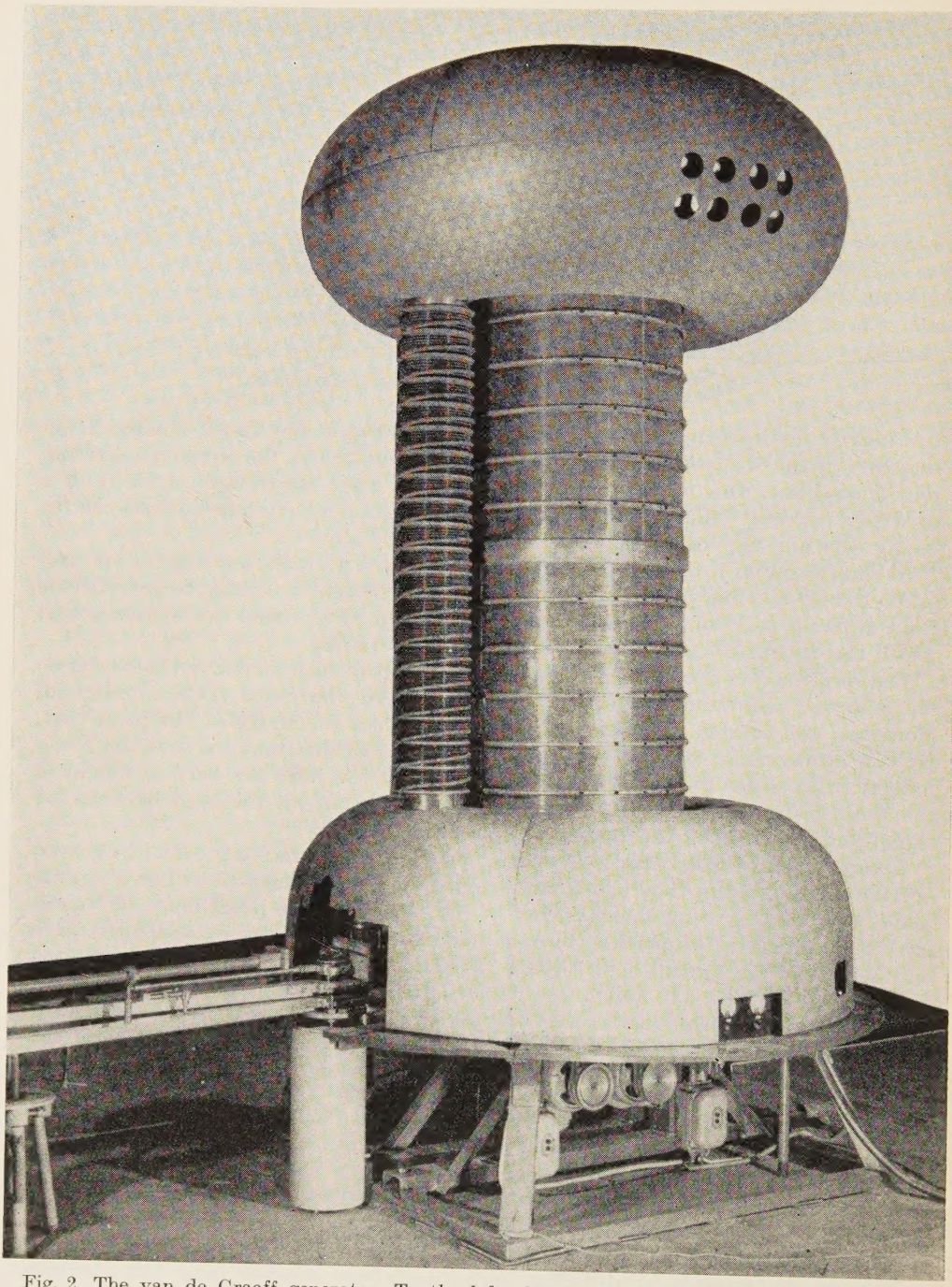

Fig. 2. The van de Graaff generator. To the left of the insulating column is the accelerating tube with the potential divider. Part of the spectrometer is seen to the left.

yielding a short circuit current of 600–700 μA. The highest obtainable voltage is about 800 kV at 300 μA electron beam.

The accelerating tube consists of 20 porcelain insulators separated by aluminium plates, which support funnel-shaped electrodes. Along the whole accelerating tube there is mounted a resistor chain in order to obtain a stabile voltage distribution. This chain contains 400 ordinary radioresistors of 20 MΩ each. The current through these resistors is measured by a μA meter on the control panel in order to get a rough value of the high voltage.

The electron gun has been previously described, OHLIN, BECKMAN [1949]; only the electric feeding has been changed. The filament is made of 0.25 mm diam. tungsten wire. The first anode immediately in front of the filament has a constant voltage of 300 V relative to the filament. The next anode is an electrode of the same kind as those in the accelerating tube. This anode is connected to a variable high tension set of max. 10 kV. In addition, the high voltage conductor of the machine contains an AC generator for 220 V, 2 A, 50 c, driven by one of the upper rollers. Filament current and focussing voltage can be controlled from the earth side by means of nylon cords that operate variable transformers in the high voltage terminal.

2. The voltmeter

The problem of measuring the voltage of van de Graaff generators is a difficult one. It is necessary to use an instrument whose load on the machine is a minimum. The most widely used instrument is the generating voltmeter, in which a sectory rotor alternately screens and unscreens stator plates. An AC signal proportional to the electric field is thus induced on the plates. The generating voltmeter used here is of a different type, in which the moving system is vibrating instead of rotating, BECKMAN [1949]. The vibrating type has the advantage that one can use higher frequencies for the AC signal and that it is easier to give this signal a sine form. The instrument employs an ordinary loudspeaker, from which the cone has been removed. Attached to the coil is a small circular plate exposed to the field from the high voltage terminal.

A small AC voltage is induced on the vibrating plate. Immediately in front of the plate is a grid, which can be given a suitable DC potential, thus compensating the field from the van de Graaff and making the AC signal zero. The grid potential at compensation is directly proportional to the field strength and consequently to the van de Graaff voltage. The grid voltage is stabilized within 0.2 per cent. The AC signal from the moving plate is amplified and rectified in a phase-sensitive rectifier. The signal can be read on a meter, which indicates the degree of compensation. The sensitivity of the meter is such that full scale deflection to each side indicates a deviation of the high voltage by about 1 per cent.

The rectified signal is used also for stabilization of the van de Graaff voltage. The signal is put on the grids of two 2A3 tubes which control the primary current to the spray voltage set. This type of stabilization is not very rapid, but it has worked well, and the high voltage could be kept constant within 1 per cent for a long period of time.

3. Target arrangements

The target-plate *1* (Fig. 3) is tightly screwed to a water-cooled copper block *2* at the bottom of a tube. The electron beam passes through a 5 mm wide aperture *3*

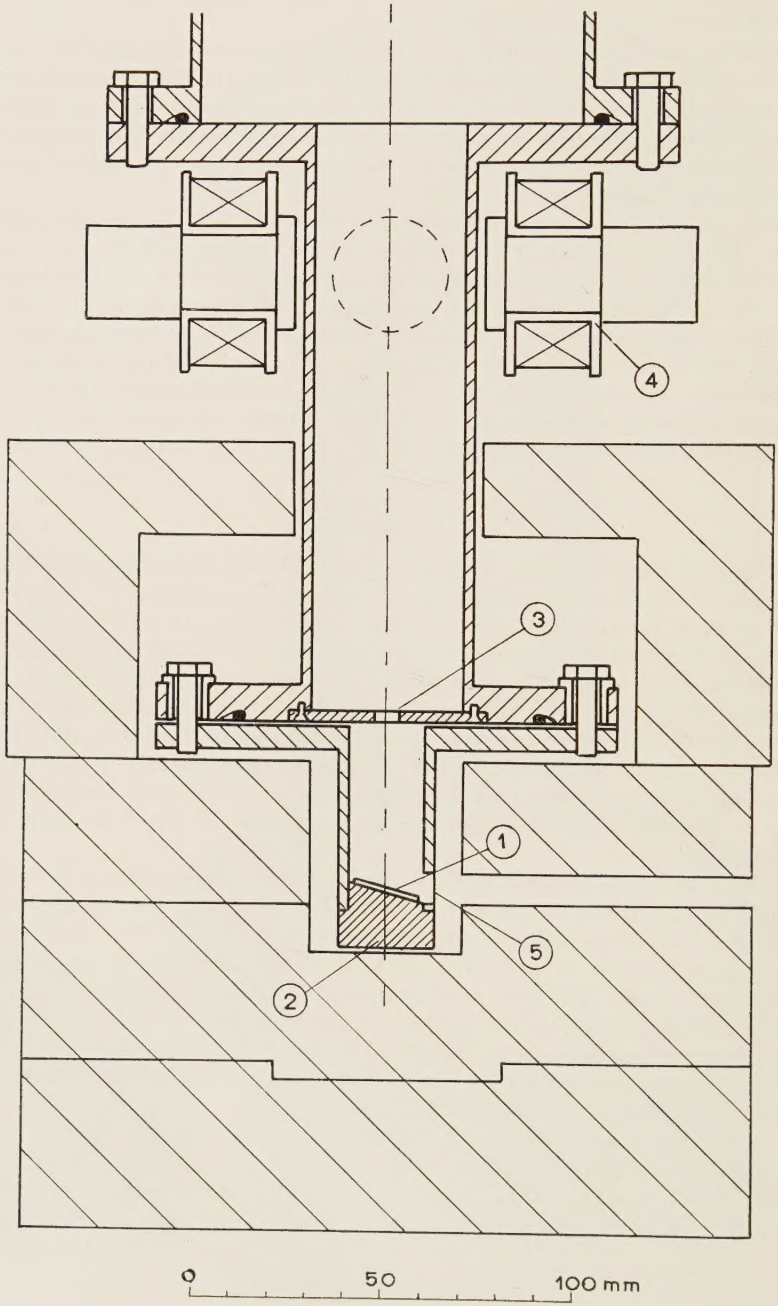

Fig. 3. The lower part of the accelerating tube showing the target arrangement and lead shields.

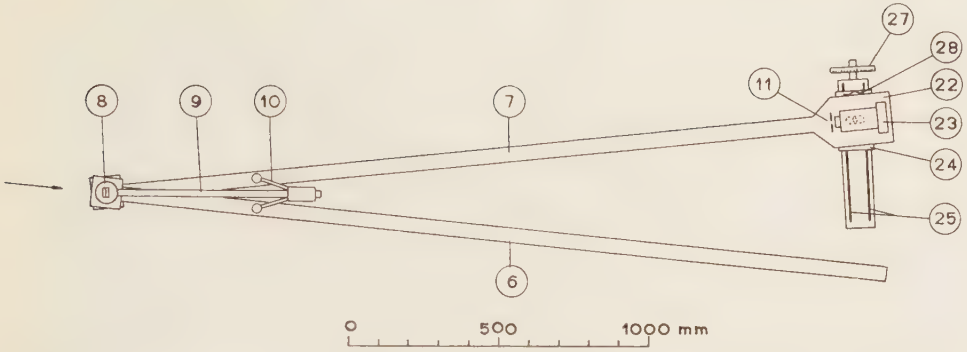

Fig. 4. Schematic drawing of the spectrometer. The arrow to the left indicates the incoming X-ray beam. The curved crystal is seen at *8*; *11* is the spectrometer slit and *23* the scintillation counter.

in a well-cooled copper plate. Two pairs of coils *4* produce two crossed magnetic fields in a plane perpendicular to the beam. By varying the currents in these coils it is possible to direct the beam through the hole *3* down to the target. The voltages on the two pairs of coils are further connected to the horizontal and vertical deflection plates in a small oscilloscope on the control panel. Thus it is easy to control the position of the focal spot continually during the measurements. The X-ray beam passes through a window *5* of 0.1 mm brass. Because of the intense X-radiation, the target and the lower part of the accelerating tube must be well shielded with lead blocks. In these blocks there is a channel of 8 × 20 mm cross-section for the X-ray beam.

For target materials, Ta, W and U were available as 1 mm thick plates. The Ir, Pt and Th samples consisted of 0.2 0.3 mm thick foils. In the latter cases it was necessary to use a copper plate as a distance piece in order to get the focal spot at the right height. Au, Tl, Pb and Bi were fastened to copper plates. The Hg target consisted of silver amalgam packed in a depression in a copper plate. Some mercury evaporated when the electron beam hit the target and the line intensities gradually decreased to about 80 per cent of the initial value during the measurements. This makes of course the intensity values for Hg more uncertain than for the other elements, but the evaporation occurred at a constant rate, so that it was possible to correct for it. Re and Os could be obtained only as metal powder, which was pressed into scores in copper plates. All the targets used were thick enough to stop the 500 keV electrons.—The vacuum system was evacuated to about 10^{-5} mm Hg by a mechanical pump and two oil diffusion pumps.

4. The current integrator

The X-ray intensity is measured relative to a constant electric charge falling on the target. Since the electron beam fluctuates a little, it is necessary to integrate the target current. The current charges a capacitor, which is discharged by an electronic circuit whenever the total charge on the capacitor reaches a predetermined fixed amount. Thus at each discharge one obtains a pulse corresponding to this fixed amount of charge. The latter must not change over a considerable period of time and must be independent of target current (within the limits of the normal fluctuations).

The integrator used is in principle the same as the one described by Elmor and

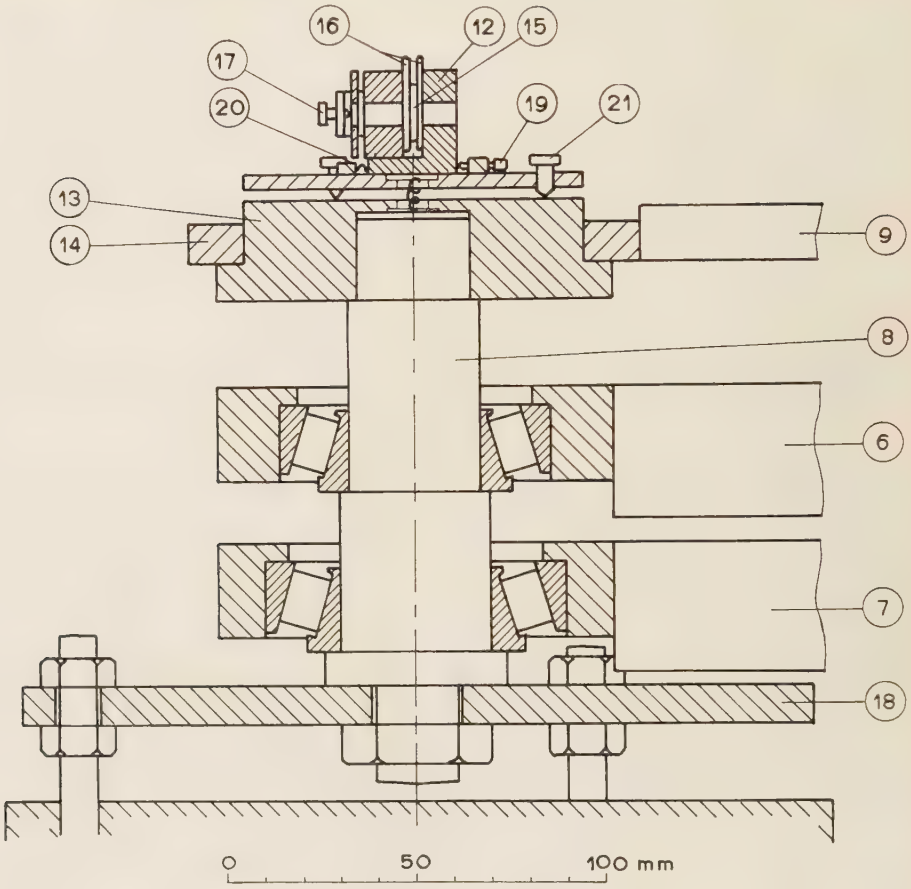

Fig. 5. The spectrometer axis with the mounting of the aluminium beams and the crystal table.

SANDS [1949] p. 405. The circuit was changed a little to register negative currents. The integrator shows very good stability and is reliable within some tenths of a per cent. Each pulse means about 2 μ coulomb.

The pulses from the integrator are counted by a Philips predetermined count scaler PW 4035. This scaler also gives pulses to switch on and off the electronics registering the X-ray intensity.

5. The spectrometer

The principal construction of the spectrograph is shown in Fig. 4. One end of each of two aluminium beams *6* and *7* are pivoted on a common vertical axis *8*. The steel rod *9* also pivoted on the axis *8*, coincides with the bisector of the angle between the aluminium beams. This is accomplished by the link system *10*. The beam *6* is fixed in the direction of the primary X-ray beam and the rod *9* is clamped to the crystal table, so that the crystal normal falls along the rod. Radiation of the wavelength

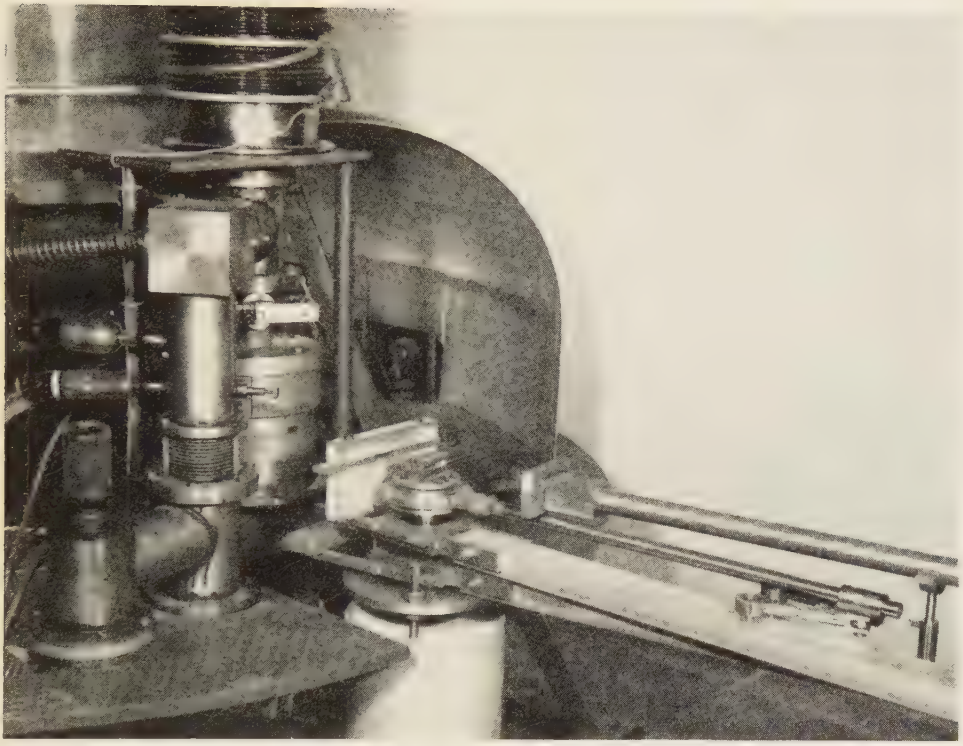

Fig. 6. Part of the spectrometer. In the middle, the crystal holder and the steel rod with the coupling links to the right. Above this coupling is the brass tube for the shielding of the diffracted X-ray beam. To the left, the accelerating tube and beneath this the lead shield at the target with the exit hole for the X-radiation.

that satisfies the Bragg equation will thus be directed along the beam *7* and focussed on the slit *11*. In every position of the spectrometer the same central part of the crystal is used for reflection. The vertical axial support *8* (Fig. 5) is mounted on an iron plate *18*, which can be leveled by means of the nuts on three bolts, cast into a concrete pillar. The two beams *6* and *7* are connected to the axis *8* by means of conical roller bearings. The crystal-holder *12* is placed on a brass block *13*, which also can rotate around the axis *8*. The steel bar *9* can be clamped to this brass block by means of the ring *14*.

The crystal holder is of the type described by BROGREN [1951]. The quartz crystal *15* is curved between two pairs of steel pins *16*, fitted in grooves in two brass blocks. The pressure at the crystal and consequently also the curvature of the crystal can be controlled by the screws *17*. The four pins are strictly parallel to each other. With this crystal holder it is possible to bend the crystal to an arbitrary radius and yet obtain good focussing conditions.

The crystal holder is clamped to the crystal table by means of two screws *19* and a spring *20*. The crystal table is then fixed to the brass block *13* by a spring and three screws *21*, so that the table can be tilted a small angle in any direction.

The link system (Figs. 4, 6) must be constructed with the utmost precision. The

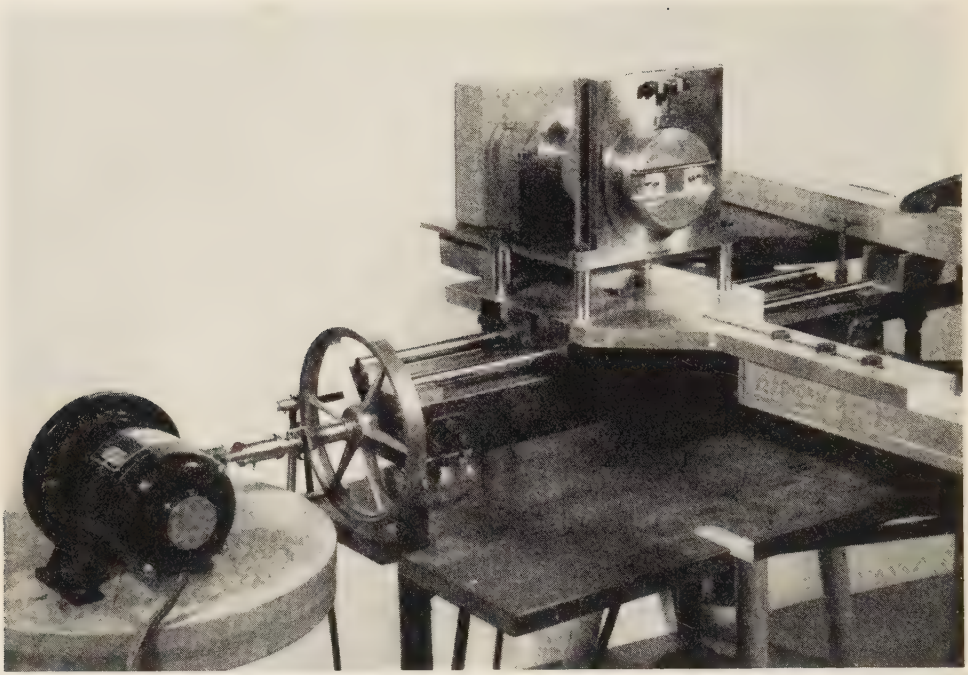

Fig. 7. Part of the spectrometer with the scintillation counter. All lead shields are removed in order to show the mounting of the spectrometer slit with the scintillation counter behind. To the right, the fixed aluminium beam *6* and the movable beam *7*. (The figures *6* and *7* refer to Fig. 4.) The beam *7* can be moved by the motor (left).

two links *10* are mounted on the beams *6* and *7* by means of ball bearings. The other ends of the links are connected to a common pivot on a coupling, which is free to move along the well-ground steel bar *9*. The lengths of the links and the distance from the ball-bearing pivots to the center *8* can be adjusted so that the steel rod always bisects the angle between the aluminium beams.

The reflected X-ray beam is directed along the beam *7* (Fig. 4) and focussed on the slit *11*, mounted in a holder which is screwed to the aluminium plate *22*. As the beam is moved, radiation of successive wavelengths passes through the slit into the scintillation counter *23*. The plate *22* rests on a brass plate *24* sliding on two steel rods *25*. The brass plate can be moved by means of a precision screw with a pitch of 1 mm. The position of the slit is read on a mm scale and on the wheel *27*, marked with a scale of 500 divisions. The screw is driven slowly by a motor (Fig. 7). The plate *24* is supplied with a short pin that fits into a slot in the upper plate *22*. A slot is necessary, because the upper plate moves along an arc of a circle, while the lower plate moves along a straight line. By means of the spring *28* the upper plate is pressed against the pin.

The scintillation counter is surrounded on all sides by 5 mm lead in order to minimize stray radiation. This lead shield has a considerable weight, and in order to decrease the load on the steel rods and on the precision screw, the lead shield is balanced by a counter weight connected to the shield by a wire laid over two pulleys.

Because of the short wavelengths the spectrometer slit must be made of a heavy

element. The jaws of the slit consist of two gold plates, 1 mm thick, soldered to pieces of silver, also 1 mm thick. The silver absorbs the K-radiation from the gold. The jaws of the slit are further shielded by two lead blocks. The slit is mounted within a ring to which is attached a short lever, as shown in Fig. 7. By means of two screws the slit thus can be rotated until it is parallel to the spectral lines.

6. The scintillation counter

A scintillation counter is a very suitable detector for the X-radiation. If the counter is combined with a single channel discriminator, the radiation of energies other than that of the X-ray lines is discarded, and in this way it is possible to maintain a very low background.

The scintillation counter used in these experiments contains a cylindrical NaI crystal, 25 mm in diameter and 25 mm high. Such a crystal registers radiation of energies up to about 300 keV with almost 100 per cent efficiency. The NaI crystal is enclosed in a thin-walled aluminium box, supplied with a glass window, which is in direct contact with the photomultiplier. MgO is used as a reflector.

The photomultiplier used is an EMI 6260, operated at 90 V per stage. The pre-amplifier, with one 6AK5 tube as cathode follower, is placed in the same cage as the multiplier tube. The pulses are led through a 4 m long coaxial cable to a linear amplifier, Model 100 (Elmor and Sands [1949]), at the control panel. The single channel discriminator (Aström, [1954]) selects the amplified pulses which have a size corresponding to the energy of the K-radiation. The pulses are recorded by a scale-of-64 (Atomic Instrument Company Model 101-A). Since, on the one hand, pulses from a scintillation counter are very short (about 1 μ sec) and, on the other, the counting rates never exceeded 300 pulses per second, there was no problem of dead-time corrections.

7. Shielding

The scintillation counter must be very carefully shielded against stray radiation in order to decrease the background. The high energy of the electron beam (500 keV) and the small angle between the direct and reflected X-ray beam (minimum angle 6°) make the difficulties of shielding rather great. Fortunately, because of the use of the channel discriminator, which discards all pulses of energy different from that of the registered K lines, the demands on shielding are not so high as would be the case if, for instance, a GM tube was used. On the other hand, extra pulses of wrong energy in the scintillation counter are, of course, not desirable.

The target itself is placed at the center of a lead block, 20 cm in diameter and 20 cm in height, with a small channel for the X-ray beam. The parts of the vacuum system above the target are shielded by 5–10 mm lead.

A rather strong radiation, however, comes from the lower parts of the accelerating tube because of stray electrons. Furthermore, secondary X-rays may be emitted from most parts of the machine. In order to avoid this rather weak radiation, the reflected beam is guided through a brass tube extending almost the entire distance from the crystal to the counter slit, as shown in Figs. 2 and 6. The scintillation counter is placed in a lead housing made of 5 mm lead with an extra lead shield on the front side.

In this way it has been possible to eliminate almost all stray radiation. Only about 30 per cent of the background in the registered curves is attributable to stray radiation, probably largely arising from scattering in the crystal holder.

CHAPTER III

Recordings with the spectrometer

1. Adjustment

1. The crystal holder was placed at the same height as the target. By pinhole camera photographs of the focal spot it was checked that the line from the center of the focal spot through the center of the crystal holder was horizontal.

2. The aluminium beam *6* in Fig. 4 was adjusted horizontally and fixed in the direction of the primary X-ray beam.

3. The crystal was placed in the holder and bent to approximately the desired radius (about 2.5 meters). A slit lamp was placed on the beam *6* and the image of the slit reflected by the crystal used as a concave mirror, was examined.

4. When the crystal was bent satisfactorily, the exact focus was determined by examining the sharpness of X-ray lines recorded on films placed at every 10th centimeter on both sides of the assumed focus.

5. The axis *8* was made vertical and by means of a centering microscope the crystal was adjusted so as to have its center on the axis *8*.

6. By means of adjusting screws at the table carrying the scintillation counter the beam *7* was leveled horizontally. At the same time the rods *25* were adjusted horizontally.

7. The surface of the crystal was made parallel to the rotation axis by the adjusting screws *21*.

8. The link system was now adjusted so that the image of the slit lamp placed on the beam *6* coincided with the counter slit for all positions of the spectrometer. The rod *9* was then the bisector of the angle between the aluminium beams.

9. The spectrometer slit was set parallel to the X-ray lines. An X-ray film was placed in front of the slit and illuminated from behind for a moment. On the same film X-ray lines were also exposed. By examination of the film in a microscope it was possible to determine the angle between the two images.

10. On a film placed in front of the slit two X-ray spectra were exposed with the crystal in two different positions. At the same time several exposures were made of the counter slit. It was thus ascertained that the spectrum lines and the slit were moving parallel to each other.

The radius of curvature of the quartz crystal ($22\bar{4}3$) was 2660 mm. This curvature resulted in a linear dispersion of 0.382 XU/mm. Because of the small reflecting angles ($< 6°$) the dispersion can be assumed constant through the whole wavelength region, and the spectrometer readings in mm could be set proportional to the wavelength in XU. The length of the spectrometer screw was 200 mm and thus a wavelength region of 76 XU could be covered at one time. The spectrometer was first adjusted for the wavelength region 150-225 XU and then for the region 100-175 XU. In both regions the steel rods *25* (Fig. 4) were adjusted perpendicular to the aluminium beam *7*, when the spectrometer was set at the middle of the wavelength region.

The slit width was 0.1 mm and the height of the slit 15 mm. The approximately circular focal spot had a diameter of 5 mm. Since the angle between the target surface and the horizontal plane was 15°, the vertical dimension of the focal spot was only 2 mm. This involves only a negligible broadening of the spectral lines under the geo-

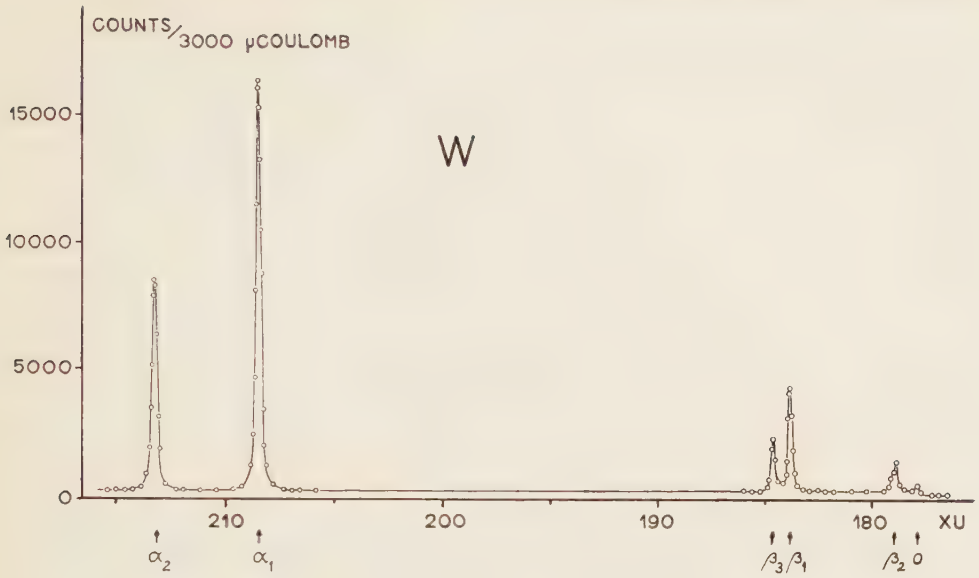

Fig. 8. General view of tungsten K-spectrum.

metrical conditions prevailing. Furthermore it is evident that only a small central part (2 × 5 mm) of the crystal was used for reflection. The quartz crystal had the dimensions 1 × 15 × 25 mm and the aperture of the crystal holder was 6 × 13 mm. It was thus easy to avoid screening of the X-ray beam by the crystal holder.

2. Procedure

During the measurements the channel discriminator must be set at a pulse-height that corresponds to the energy of the X-ray line being measured. Prior to each run the spectrometer was set at the peak of either the α_1 or β_1 lines and the pulse spectrum was recorded by varying the channel discriminator. In this way a curve with a flat top was obtained and from this curve the discriminator setting was determined. Such pulse spectra were always taken for the α_1 and β_1 lines. The electronic circuits were found to be very stabile, and the discriminator setting was almost the same from one day to another for the same line.

When recording an X-ray line the scintillation counter was switched on for the time during which the charge was registered by the integrator. The integrator counted from about 300 to 3000 pulses for each point, depending on the intensity of the X-radiation. The van de Graaff voltage was maintained at 500 kV for all spectrograms, and the electron beam current was about 80 μA. Only the most intense lines α_1 and α_2 sometimes required a decrease in the electron beam current in order to avoid too high counting rates.

Chapter IV

Computation of the X-ray intensities

Fig. 8 shows the general appearance of a complete spectrum. Since the spectra of all elements are very similar, the spectrum of only one element, tungsten, is published.

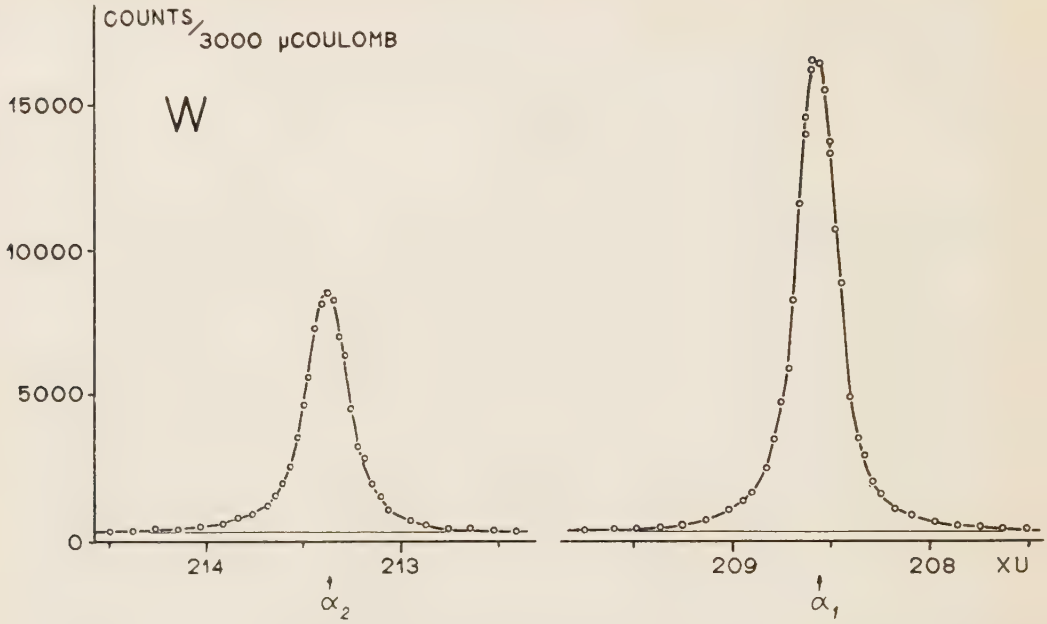

Fig. 9. Tungsten K-spectrum. The α lines.

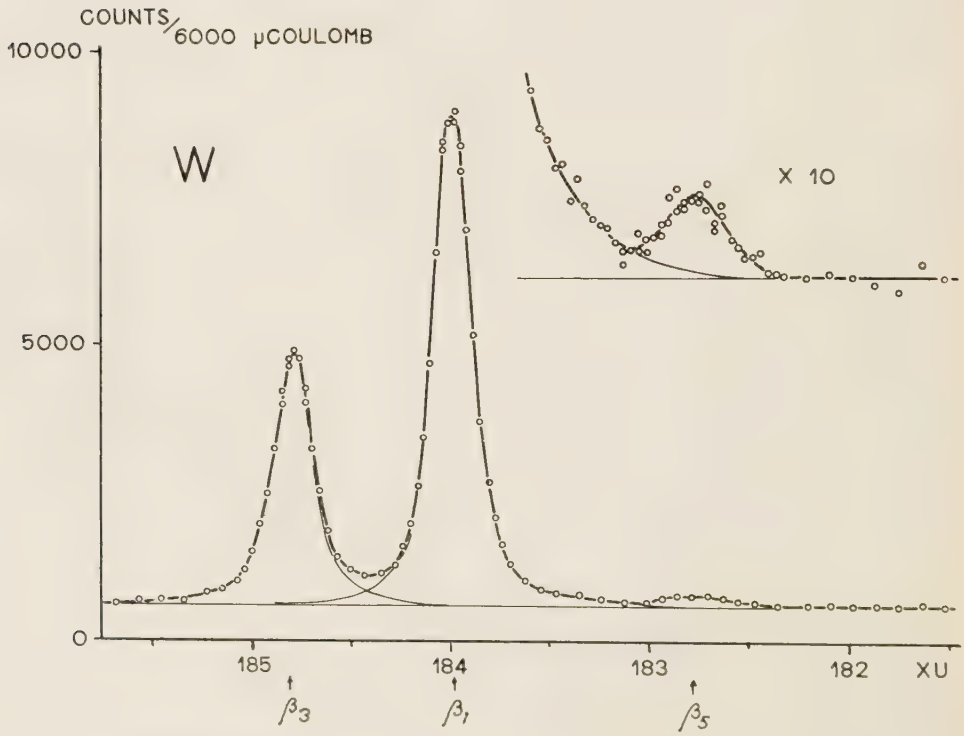

Fig. 10. Tungsten K-spectrum. The dipole lines β_1 and β_3 and the quadrupole line β_5

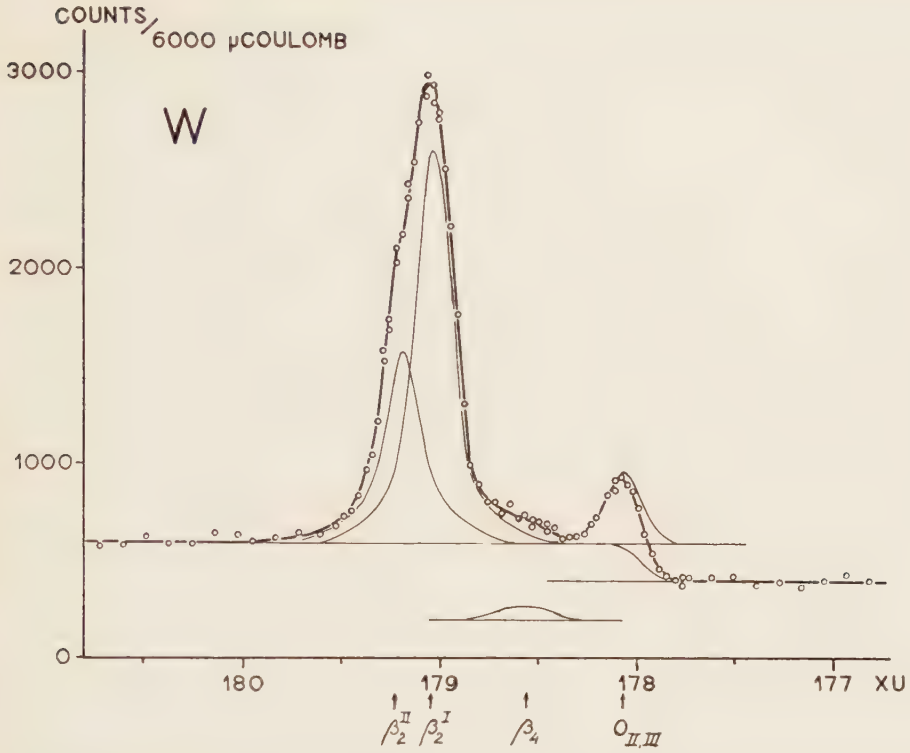

Fig. 11. Tungsten K-spectrum. The β_2 line resolved in its components, the $KO_{II,\,III}$ line and the K-edge. Between the β_2 and $KO_{II,\,III}$ lines is seen the weak quadrupole line β_4.

The details of the tungsten spectrum are seen in Figs. 9, 10, 11. The registered spectra were plotted on a large scale and the areas under the curves measured by means of a planimeter (G. Coradi, Zürich). Before the planimeter measurements were made, the background was drawn in as a straight line parallel to the abscissa axis. Neighbouring lines were also separated from each other. This was not difficult in the case of β_1, β_3 and β_5. The β_2 line consists of two components belonging to the transitions KN_{II} and KN_{III}. The line can be separated (see Fig. 11), but this cannot be done without some knowledge of the intensity distribution between the components and therefore only intensity values referring to the unseparated line are given. The area under the weak line β_4 was measured, but the neighbouring lines β_2 and $O_{II,\,III}$, of course, make the result very uncertain. Because the continuous radiation forming the background is partly absorbed in the target itself, there is a considerable change in the background from one side of the K-edge to the other (see Fig. 11). This change affects the profile of the $O_{II,\,III}$ line considerably. It was necessary to adopt a trial and error method for the separation of this line from the edge. In the case of tungsten the result thus obtained was confirmed by recording an ordinary absorption spectrum. A W foil of 0.1 mm thickness was put in the X-ray beam using a Pt target. The W K-edge thus obtained showed the same profile as the one separated from the $O_{II,\,III}$ line.

The lines in each of the three groups represented by Figs. 9, 10 and 11 were always measured in the same recording. The ratios of the areas of the lines in these groups are

Table 1. Measured values of the areas under the recorded curves, quartz $22\bar{4}3$.

Element	α_2/α_1	β_3/β_1	β_5/β_1	β_4/β_2	$O_{II\,III}/\beta_2$
73 Ta	0.543	0.505	0.021	0.007	0.090
	525	539	25	13	102
	537	515	24	6	74
	545	521	23	12	82
Mean	**0.538**	**0.520**	**0.023**	**0.010**	**0.087**
74 W	0.577	0.561	0.025	0.024	0.091
	529	593	21	14	113
	524	522	20	13	95
	559	558	21	14	109
	579	520	24	13	108
	542	514	22	18	98
	569	507			
Mean	**0.554**	**0.539**	**0.022**	**0.016**	**0.102**
75 Re	0.580	0.504	0.022	0.023	0.113
	502	507	30	27	102
	583	547	17	21	130
	593	538	24	18	93
Mean	**0.565**	**0.524**	**0.023**	**0.022**	**0.110**
76 Os	0.561	0.573	0.027	0.019	0.132
	536	490	22	18	102
	608	519	28	22	70
	567	508	30	33	138
Mean	**0.568**	**0.523**	**0.027**	**0.023**	**0.111**
77 Ir	0.564	0.552	0.019	0.021	0.136
	573	484	28	22	95
	543	534	27	21	136
	544	554	32		
	556				
	554				
Mean	**0.554**	**0.531**	**0.026**	**0.021**	**0.122**
78 Pt	0.577	0.513	0.025	0.024	0.104
	564	563	32	25	138
	572	534	31	18	125
	542	527	25	25	121
	531	516			
	572				
	578				
Mean	**0.562**	**0.531**	**0.028**	**0.023**	**0.122**
79 Au	0.557	0.507	0.026	0.020	0.126
	538	524	35	13	108
	543	529	28	28	139
	548	517		16	90
	525	521		16	138
	563	512			
Mean	**0.546**	**0.518**	**0.030**	**0.018**	**0.120**

Table 1 (cont.)

Element	α_2/α_1	β_3/β_1	β_5/β_1	β_4/β_2	$O_{II\,III}/\beta_2$
80 Hg	0.575	0.55	0.027		0.14
	555	45	25		23
	494				
	526				
Mean	**0.538**	**0.50**	**0.026**		**0.18**
81 Tl	0.608	0.535	0.025	0.020	0.164
	583	506	25	19	174
	583	608	25	22	175
Mean	**0.591**	**0.550**	**0.025**	**0.020**	**0.171**
82 Pb	0.608	0.585	0.027	0.024	0.146
	590	515	31	23	154
	520	539	27	26	159
	539				
Mean	**0.564**	**0.545**	**0.028**	**0.024**	**0.153**
83 Bi	0.569	0.497	0.028	0.026	0.133
	585	492	26	23	141
	600	528	33	23	139
	541				
	643				
Mean	**0.588**	**0.506**	**0.029**	**0.024**	**0.138**
90 Th	0.568	0.535	0.032	0.026	0.276
	610	493	33	57	284
	547	480	39		221
Mean	**0.575**	**0.503**	**0.035**	**0.041**	**0.260**
92 U	0.616	0.532	0.032	0.044	0.213
	595	521	38	41	254
	606	482	36	33	275
	597				
Mean	**0.604**	**0.512**	**0.035**	**0.039**	**0.247**

listed in Table 1, as they were obtained from the separate runs. Table 2 contains the ratios $\beta_{1'}/\alpha_1$ and β_2'/β_1'. These ratios could not be determined with the same accuracy as the other ratios because the lines were not registered in sequence. The difference in accuracy is small, however, since the intensity of a given line showed only small variations from one day to another (about 5 per cent).

Tables 1 and 2 contain the results obtained with the plane $22\bar{4}3$. The tungsten spectrum was also measured employing the plane $13\bar{4}0$ (Table 3). As shown there, the two crystal planes give the same values of the relative intensities, indicating that the reflecting properties of the two crystal planes are the same.

The peak intensities of the registered lines can be used for computation of intensity ratios if the lines are of the same width which is approximately the case for the K lines. The peak intensity of the strongest lines α_1, α_2, β_1 and β_3 was measured (Table

Table 2. Measured values of the areas under the recorded curves, quartz $22\bar{4}3$.

Element	β_1/α_1	β_2/β_1
73 Ta	0.227	0.311
74 W	0.228	0.334
75 Re	0.223	0.337
76 Os	0.225	0.340
77 Ir	0.216	0.309
78 Pt	0.217	0.356
79 Au	0.225	0.328
80 Hg	0.23	0.36
81 Tl	0.220	0.399
82 Pb	0.222	0.369
83 Bi	0.226	0.360
90 Th	0.227	0.397
92 U	0.220	0.412

Table 3. Measured values of the areas under the recorded curves, quartz $13\bar{4}0$.

Element	α_2/α_1	β_3/β_1	β_5/β_1	β_4/β_2	$O_{II\,III}/\beta_2$	β_1/α_1	β_2/β_1
74 W	0.527	0.545	0.022	0.019	0.092		
	510	553	23	16	83		
	539	505					
	558						
Mean	**0.534**	**0.534**	**0.022**	**0.018**	**0.088**	**0.226**	**0.334**

Table 4. Measured peak values of the recorded lines, quartz $22\bar{4}3$.

Element	α_2/α_1	β_3/β_1	β_1/α_1
73 Ta	0.529	0.502	0.235
74 W	0.537	0.520	0.252
75 Re	0.547	0.513	0.230
76 Os	0.560	0.519	0.235
77 Ir	0.553	0.500	0.232
78 Pt	0.543	0.514	0.237
79 Au	0.525	0.502	0.246
80 Hg	0.538	0.53	0.24
81 Tl	0.572	0.515	0.229
82 Pb	0.544	0.531	0.226
83 Bi	0.573	0.526	0.234
90 Th	0.563	0.536	0.235
92 U	0.608	0.517	0.232

4). The other lines of the spectrum are double, and a separation into the components in order to determine the peak intensities cannot possibly be carried out with any accuracy. A comparison between the peak and the area values shows that there is a marked difference only for the β_1/α_1 ratio. The difference (about 5 per cent) may be attributed to the different width of the α and β lines.

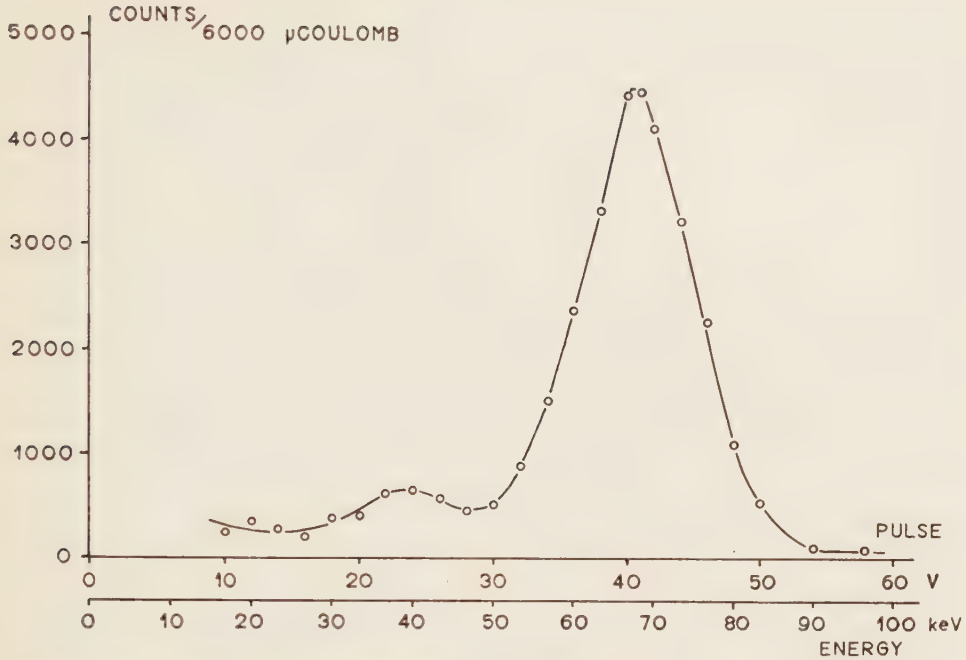

Fig. 12. Pulse spectrum of the scintillation counter; the spectrometer set at the Au $K\alpha_1$ line. Channel width 3 volts. The photopeak is at 69 keV, and the iodine K-escape peak at 40 keV.

In calculating the relative transition probabilities and intensities of the X-ray lines from the experimentally determined quantities, it is necessary to take several factors into consideration. The ratio of the intensities of two lines may be influenced by the following factors:

1. Varying efficiency of the scintillation counter at different wavelengths.
2. Absorption of the X-ray beam from the target to the counter.
3. X-ray absorption in the target itself.
4. Reflection properties of the quartz crystal.

The absolute intensity of an X-ray line is greatly influenced by these factors, but the relative intensity values are influenced only if these factors depend on the wavelength. It was found necessary to correct the experimentally determined intensity ratio only when the lines differed greatly in wavelength. The corrections were in general appreciable only for the ratio between the β_1 and α_1 line intensities and were usually negligible in other cases.

1. The efficiency of the scintillation counter

Fig. 12 shows a typical pulse spectrum from the scintillation counter, when the spectrometer was placed at the Au $K\alpha_1$ line. The channel width was 3 volts. The diagram shows that about 90 % of the radiation is detected at the right pulse height (the photopeak). The small peak of lower energy is the iodine K-escape peak. The incoming quantum has excited the K-shell in an I atom and the emitted K-radiation

Table 5. Correction factors for the ratio β_1/α_1.

Element	Escape prob.	Absorption, X-ray beam	Absorption, target	Crystal refl.
73 Ta	0.98	0.96	0.79	1.29
79 Au	0.98	0.97	0.83	1.29
82 Pb	0.98	0.98	0.84	1.28
92 U	0.99	0.99	0.89	1.28

has escaped from the NaI crystal. The difference between the two peaks is 29 keV which is in agreement with the energy of the K lines of iodine.

When the scintillation counter was used in the spectrometer, the channel width was set at 20 volts. Thus the whole photopeak was utilized and about 90 per cent of the X-radiation was recorded by the counting devices. The wide channel has the advantage that the pulse spectrum shows a flat top, almost a plateau, which makes the discriminator setting less critical. A change of 1 volt corresponds to a change of less than 1 per cent in the registered X-ray intensity. Since only the part of the radiation that corresponds to the photopeak is registered in the spectrometer, it is necessary to know the iodine escape probability and how it changes with the energy of the X-ray quanta.

Complete pulse spectra with a narrow channel were registered for the α_1 lines of tungsten, gold and thorium (photon energies 59.2, 68.7 and 93.2 keV). The escape probability thus obtained (10.9, 9.7 and 3.6 per cent respectively) is in agreement with the results of other investigators, LIDÉN and STARFELT [1954], AXEL [1954] and MEYERHOF and WEST [1954]. The variation of escape probability with photon energy introduces only small corrections to the intensity ratios. (Table 5.)

2. Absorption of the X-ray beam

The X-rays are subject to absorption at the following points: (1) the window of the vacuum system, (2) the quartz crystal, and (3) the aluminium container for the NaI crystal of the counter.

The correction necessary as a result of these effects is greatest for Ta and decreases to very small values for U. The total correction, calculated for β_1/α_1, for several elements is shown in Table 5. The main part of the correction arises from absorption in the X-ray tube window (0.11 mm brass). The absorption in the air is negligible.

3. X-ray absorption in the target

The absorption in the target is due to the penetration of the electrons into the target with the result that the X-rays are emitted from different depths. The emitted X-rays are partly absorbed by the target to an extent that is rather wavelength dependent. The correction that must be applied is very difficult to calculate. The method used here is similar to the one used by WILLIAMS [1933]. The problem is discussed also by COMPTON and ALLISON [1935] in detail.

The electrons are assumed to go in a straight path into the target, at the same time being successively retarded. The X-rays under consideration are emitted at an angle of 90° to the electron beam. Atoms excited by electron impact at the depth x (meas-

ured in the direction of the electron beam) emit X-ray quanta that pass through target material for a distance $\frac{x}{\operatorname{tg}\alpha}$ where α is the angle between the X-ray beam and the target surface. The number of quanta dN_λ at the target surface emitted from the part dx of the electron beam is

$$dN_\lambda = k \cdot T_\lambda \cdot F(U) \cdot e^{-\frac{\mu_\lambda \cdot x}{\operatorname{tg}\alpha}} dx, \tag{1}$$

where k is a constant, T_λ the radiation transition probability for quanta of wavelength λ, μ_λ the absorption coefficient of the target material and $F(U)$ the ionization function for K-excitation. U is the energy of the electrons measured in units of K-excitation energy. Integrating from the target surface to the depth x_0, at which the electron energy is just equal to the K-excitation energy of the target material, gives the total number of emitted X-ray quanta in the appropriate direction,

$$N_\lambda = k \cdot T_\lambda \int_0^{x_0} F(U) \cdot e^{-\frac{\mu_\lambda \cdot x}{\operatorname{tg}\alpha}} dx. \tag{2}$$

$F(U)$ has been measured by WEBSTER, HANSEN and DUVENECK [1933] who give the following equation as a good fit for the experimentally determined values:

$$F(U) = \text{const.} \frac{6}{U\left[\left(\frac{\pi}{2 \arccos\sqrt{\frac{1}{U}}}\right)^2 - 1\right]}. \tag{3}$$

In addition it is necessary to know U as a function of x, that is, the electron energy at various depths in the target. Experimental data on the stopping of electrons in matter are obtained from GOODMAN [1947] and SIEGBAHN [1955]. The values of the X-ray absorption coefficient are given by VICTOREEN [1949]. It is necessary to evaluate the integral (2) graphically. The corrections thus obtained are listed in Table 5 for the ratio β_1/α_1.

The above calculation of the target absorption involves two simplifying assumptions. No account has been taken of the scattering of the electrons in the target since the electron path is assumed to be a straight line, and the target atoms are assumed to be excited only by electron impact. The latter is a rather severe assumption, since photoexcitation is certainly important too. These effects are, however, very difficult to calculate.

Because of the uncertainties in the calculated target corrections it seemed wise to verify them experimentally. For that purpose, the α_1 and β_1 lines were recorded with different target arrangements. Besides the thick target with $\alpha = 15°$ used throughout the investigation, in these cases a thick target with $\alpha = 45°$ and a thin target with $\alpha = 15°$ were tried. The thick target with $\alpha = 45°$ requires a smaller correction than a target with $\alpha = 15°$. The thin target consisted of a 5 μ layer of gold evaporated on copper. In such a thin target the X-ray absorption in the gold layer is negligible. Table 6 contains the experimental values of the β_1, α_1 ratio for the three cases, and

Table 6. Experimental values of the ratio β_1/α_1 for various gold targets.

	Thin target	Thick target $\alpha = 45°$	Thick target $\alpha = 15°$
	0.181	0.207	0.221
	0.205	0.217	0.232
	0.192	0.221	0.227
Mean	**0.193**	**0.215**	**0.227**

Table 7. Correction factors for target absorption; gold β_1/α_1.

	Thick target $\alpha = 45°$	Thick target $\alpha = 15°$
Exp.	0.90	0.85
Theor.	0.93	0.83

from these figures the correction for thick gold targets are calculated. The corrections thus obtained agree within the limits of error with the theoretically estimated values as shown in Table 7.

4. Reflection properties of the quartz crystal

An X-ray line profile, as it is obtained from the spectrometer recording, is composed of the X-ray line itself and the diffraction pattern of the curved crystal. Suppose the true X-ray line can be described by the function $f(x)$ and the crystal pattern by $g(x)$ where x is a variable proportional to the spectrometer scale readings. At the small reflecting angles used here, the wavelength values, the spectrometer readings, and the Bragg angles all can be assumed to vary linearly with each other. The recorded line is then described by the function $F(x)$,

$$F(x) = \int_{-\infty}^{\infty} f(\xi)\, g(x-\xi)\, d\xi . \tag{4}$$

The total number of quanta falling into the counter when recording a line is expressed by

$$\int_{-\infty}^{\infty} F(x)\, dx = \int_{-\infty}^{\infty} \int_{-\infty}^{\infty} f(\xi)\, g(x-\xi)\, d\xi\, dx . \tag{5}$$

This expression can be rearranged to

$$\int_{-\infty}^{\infty} F(x)\, dx = \int_{-\infty}^{\infty} f(\xi)\, d\xi \left[\int_{-\infty}^{\infty} g(x-\xi)\, dx \right] \tag{6}$$

which is equal to

$$\int_{-\infty}^{+\infty} F(x)\,dx = \int_{-\infty}^{+\infty} f(\xi)\,d\xi \cdot \int_{-\infty}^{+\infty} g(x)\,dx. \tag{7}$$

The different integrals can be expressed by M, T and R

$$M = T \cdot R, \tag{8}$$

where M is the total number of quanta reflected by the crystal. Since the slit geometry is the same for all positions of the spectrometer, M is proportional to the area under the curves obtained from the records. T is the number of quanta falling into the crystal under certain geometrical conditions. T is proportional to the probability of the emission of quanta belonging to a certain transition in the atom. R, which is known as the integrating reflection coefficient of the crystal, is the area under the diffraction pattern of the crystal, when a monochromatic and parallel beam of X-rays is falling into it. The ratio of the emission transition probabilities of two lines can therefore be expressed by

$$\frac{T_1}{T_2} = \frac{M_1}{M_2} \cdot \frac{R_2}{R_1} \tag{9}$$

provided that the geometrical conditions are constant, which is true in the actual spectrometer arrangement used here. It is obvious that the variation of the reflection coefficient with wavelength must be known. A thorough investigation of the reflection properties of quartz crystals has been made by Lind, West and DuMond [1950] in connection with their work on the two-meter curved crystal gamma-ray spectrometer. In the theoretical part of their paper they treat the cases of a thick perfect crystal and a mosaic crystal with low primary and secondary extinction. The reflection coefficient for a perfect crystal is:

$$R = \frac{r_0 \cdot d \cdot K}{2 \cos \theta_0} \cdot \frac{|F_H|}{V} \cdot \lambda, \tag{10}$$

and for a mosaic crystal

$$R = \frac{r_0^2 \cdot d \cdot K^2 \cdot a}{\cos^2 \theta_0} \cdot \left(\frac{|F_H|}{V}\right)^2 \cdot \lambda^2. \tag{11}$$

Here r_0 equals e^2/mc^2, d is the lattice constant for the crystal plane in question, K is the polarization factor for the X-rays, F_H the crystal structure factor and V the volume of the unit cell. The crystal has the thickness a and the Bragg angle for radiation of wavelength λ is θ_0. The conditions of low primary and secondary extinction are certainly fulfilled at the short wavelength in question.

Lind, West and DuMond studied the reflection properties of the $13\bar{4}0$ plane of quartz in the wavelength region 500 to 9 XU. Their measurements show a variation of R with λ^2 which is an indication that quartz behaves as a mosaic crystal when it is elastically bent. Their measurements on an unstressed crystal plate show that this behaves more nearly as a perfect crystal.

Since their results obviously indicate that an elastically bent quartz crystal reflects as a mosaic crystal, the value of R from eq. (11) was adopted. Because of the small values of θ, the factor $\cos\theta$ can be assumed to be equal to 1, and the variation of the

Table 8. Radiation transition probabilities for the K lines of heavy elements relative to $K\alpha_1 = 100$.

Element	α_2	α_1	β_3	β_1	β_5	β_2	β_4	$O_{II\,III}$
73 Ta	53.6	100	11.1	21.5	0.49	6.7	0.07	0.6
74 W	54.4	100	11.8	21.9	0.48	7.3	0.13	0.7
75 Re	56.0	100	11.3	21.7	0.50	7.3	0.16	0.8
76 Os	56.3	100	11.4	22.1	0.60	7.6	0.17	0.9
77 Ir	54.3	100	11.2	21.4	0.58	6.7	0.14	0.8
78 Pt	55.0	100	11.4	21.7	0.61	7.7	0.18	0.9
79 Au	53.3	100	11.7	22.8	0.68	7.6	0.14	0.9
80 Hg	52.4	100	12	24	0.61	8.6		1.5
81 Tl	57.6	100	12.3	22.7	0.57	8.7	0.17	1.5
82 Pb	54.8	100	12.4	23.1	0.65	8.6	0.21	1.3
83 Bi	57.0	100	11.9	23.6	0.68	8.6	0.21	1.2
90 Th	55.0	100	12.4	25.1	0.88	10.1	0.41	2.6
92 U	57.5	100	12.4	24.6	0.86	10.3	0.40	2.5

Table 9. Intensities of the K lines of heavy elements relative to $K\alpha_1 = 100$.

Element	L_I[1] KL_I	α_2 KL_{II}	α_1 KL_{III}	β_3 KM_{II}	β_1 KM_{III}	β_5 $KM_{IV\,V}$	β_2 $KN_{II\,III}$	β_4 $KN_{IV\,V}$	$O_{II\,III}$ $KO_{II\,III}$
73 Ta		52.4	100	12.5	24.3	0.57	7.8	0.08	0.7
74 W	0.16	53.2	100	13.3	24.8	0.56	8.5	0.14	0.9
75 Re		54.7	100	12.8	24.6	0.57	8.5	0.19	1.0
76 Os		54.9	100	12.9	25.0	0.69	8.9	0.20	1.0
77 Ir		53.0	100	12.7	24.3	0.64	7.8	0.16	1.0
78 Pt		53.6	100	12.9	24.6	0.69	9.0	0.21	1.1
79 Au	0.22	51.9	100	13.2	25.8	0.77	8.8	0.16	1.1
80 Hg		51.0	100	13.1	26.6	0.72	10.0		1.8
81 Tl		56.0	100	13.9	25.7	0.65	10.1	0.20	1.7
82 Pb		53.2	100	14.0	26.2	0.74	10.0	0.24	1.5
83 Bi		55.3	100	13.4	26.8	0.80	10.0	0.24	1.4
90 Th		53.0	100	14.0	28.4	0.98	11.8	0.48	3.1
92 U		55.3	100	14.0	27.8	0.98	12.0	0.47	3.0

[1] Regarding the KL_I-transition, see Chapter VI, p. 526.

polarisation factor K with wavelength considered negligible. Equation (9) can thus be written:

$$\frac{T_1}{T_2} = \frac{M_1}{M_2} \cdot \frac{\lambda_2^5}{\lambda_1^5}. \tag{12}$$

The transition probabilities for emission of X-ray quanta were calculated from eq. (12) after correction for the X-ray absorption discussed in the preceding sections. In the main part of this investigation the plane $22\bar{4}3$ has been used. In the case of tungsten some measurements have been made using the plane $13\bar{4}0$ (Table 3). The intensity ratios for tungsten obtained from the two crystal planes are equal, showing that the reflecting properties are equal for the two planes.

The quantity T is proportional to the radiation transition probability, whereas

the intensity I of an X-ray line is proportional to the emitted energy. Since the energy of each quantum is $h\nu$, one has

$$I = T \cdot h\nu. \tag{13}$$

The final values of the transition probability for quantum emission are listed in Table 8, while in Table 9 are tabulated the intensity values. In each case the α_1 line is put arbitrarily equal to 100.

Chapter V

Discussion of the results

1. General remarks on *K*-spectra

The elements investigated have an electron configuration, where the four first shells (K, L, M, N) are completely filled. The N-shell is completed at 71 Lu, the last of the rare earth elements. For 73 Ta the electron arrangement is:

K-shell: $1s^2$
L-shell: $2s^2 2p^6$
M-shell: $3s^2 3p^6 3d^{10}$
N-shell: $4s^2 4p^6 4d^{10} 4f^{14}$
O-shell: $5s^2 5p^6 5d^3$
P-shell: $6s^2$

The following elements until 78 Pt are characterized by the filling of the $5d$-level. At 81 Tl the first $6p$ electrons appear, and this subshell is filled at the rare gas 86 Rn. At 90 Th the electrons enter the $5f$ subshell at the beginning of the actinide group. The outer shells at 92 U have the following configurations:

O-shell: $5s^2 5p^6 5d^{10} 5f^3$
P-shell: $6s^2 6p^6 6d$
Q-shell: $7s^2$

K-spectra are obtained if an $1s$-electron is removed and the vacancy in the K-level is filled by an electron jump from an outer level. Since the K-shell contains only one level, the K-spectra are very simple in their structure. The initial state is always an $1s^{-1}$ state with the total angular momentum 1/2 and even parity ($1/2^+$). The final states of the transitions occurring in the K-spectra have the following J-values and parities:

s	$1/2^+$
p	$1/2^-$ $3/2^-$
d	$3/2^+$ $5/2^+$
f	$5/2^-$ $7/2^-$

The radiation emitted in a transition is characterized by its multipole order L, where L combines vectorially with the quantum numbers J_i and J_f of the initial and final states of the atom. The radiation occurs with or without parity change according to the following rules:

$$\text{electric radiation} \quad (-1)^L = \pm 1$$
$$\text{magnetic radiation} \quad (-1)^{L-1} = \pm 1$$

where the result -1 means parity change and -1 means no parity change.

The strongest lines arise always from electric dipole transitions ($E1$), where $L = 1$. According to the selection rules this transition occurs between states of different parity. In the K-spectra this means transitions from the $1s$-state to a p-state, that is to the levels L_{II}, L_{III}, M_{II}, M_{III}, N_{II} N_{III}, O_{II} O_{III} and P_{II} P_{III}. The electric quadrupole ($E2$) and magnetic dipole ($M1$) transitions are considerably less probable, and the corresponding X-ray lines are very weak. $E2$-transitions give rise to the $1s$-nd lines, namely $KM_{IV,\,V}$ (β'_5) and $KN_{IV,\,V}$ (β'_4). Two s-states can only combine with $L = 1$. A transition between two s-levels, which must occur without parity change, is thus only permitted as magnetic dipole radiation ($M1$). The very faint KL_I line on the long wavelength side of the α_2 line is of this type. Electric octupole ($E3$) transitions can occur between the $1s$-level and the $4f$-level, but the line resulting from this transition is surely not detectable owing to the very small intensity.

2. Earlier investigations

A systematic study of the intensity relations in K-spectra has been made by MEYER [1929] and by WILLIAMS [1933]. MEYER has investigated elements from 23 V to 49 In, using a crystal spectrometer and the photographic-photometric method for obtaining the intensity of the lines. This includes, however, some very uncertain corrections regarding the sensitivity of the photographic plate. The intensity values given by WILLIAMS [1933] for several elements from 24 Cr to 52 Te are probably more reliable, since he used an ionization chamber as detector. Furthermore the efficiency of the detector was studied carefully and the results were corrected for X-ray absorption, for reflection properties of the crystal and for the target absorption.

With respect to the heavy elements only a few papers have appeared in the later years.[1] KLIEVER [1939] studied 74 W and 78 Pt with a double crystal spectrometer and ionization chamber. His results were corrected for the detector efficiency and the absorption of the X-ray beam, but the target correction was not estimated. The intensity relations for spectra of some heavy elements have been studied by VOTH [1942] using an absorption method. He measured the intensity of the secondary X-rays emitted from a radiator with and without different filters. The absorption filters were made of elements having their K-edges between the α and β lines as well as on the long and short wavelength side of the lines of the element used as radiator. In this way he was able to measure the intensity ratio between the α-group and the β-group for the elements 75 Re to 82 Pb. For some elements it was possible to use filters with the K-edge between the α_1 and α_2 lines or between the two β-groups of the K-spectrum of the radiator, and thus the α_2 α_1 ratio and some other intensity ratios could be determined for a few elements. This absorption method offers some advantage because of the simple experimental arrangement (no spectrograph is needed), but it is doubtful if it can give the same accuracy as the spectrometer method. Though one avoids the corrections for crystal reflection, other errors are introduced, for instance those arising from the Compton scattering in the radiator. Furthermore it is necessary to know the absorption coefficients very accurately. VOTH's results, together with those of the above-mentioned investigators, are plotted in the Figs. 13–18.

[1] Regarding earlier measurements see DUANE and STENSTRÖM [1920], SIEGBAHN [1931] and COMPTON and ALLISON [1935].

Theoretical calculations of the intensities of X-ray lines are very difficult to make because of the very complicated wave functions for the heavy elements. A calculation based on screened hydrogen eigenfunctions modified by relativistic effects has been made by PINCHERLE [1933] for 74 W and by MASSEY and BURHOP [1936] for 51 Sb, 79 Au and 92 U. RAMBERG and RICHTMYER [1937] have calculated the radiation and Auger transition probabilities for 79 Au. Their values are here converted to intensity values.

3. The present measurements

The intensities of the dipole-lines as compared with the α_1 line are plotted against Z in Figs. 13, 14, 15 and 16. The ratios β_5/β_1 and β_4/β_2 of the quadrupole line intensities to those of the neighbouring dipole-lines are shown in Figs. 17 and 18. The vertical lines marked at some points in the diagrams indicate the estimated errors including both statistical and systematic errors. The statistical errors, which depend on the uncertainty in the voltage and current integrator measurements and in fluctuations in the focal spot, amount to about 5 per cent for the stronger lines and to 10–20 per cent for the weaker ones. Systematic errors arise mainly from target correction and crystal reflection factors. In the case of the $KO_{II,III}$ line errors are introduced because of the K-edge, which strongly affects the profile of the line. As earlier pointed out, the separation of the line from the edge is very difficult to make since the shape and wavelength value of the edge is not accurately known. Further the target correction for the line is difficult to calculate because of the abrupt change in the absorption coefficient for the target material at the K-edge. The correction applied here is the same as for the β_2 line, which might cause the $KO_{II,III}$ line intensities to be some per cent too low.

a) The dipole lines

As mentioned above the dipole lines arise from electron jumps from levels $L_{II,III}$, $M_{II,III}$, $N_{II,III}$, $O_{II,III}$ and $P_{II,III}$ to the K-level. Transitions to the L- and M-levels result in the well separated doublets $\alpha_1\,\alpha_2$ and $\beta_1\,\beta_3$. The β_2 line ($KN_{II,III}$) shows marked asymmetry and can be resolved into its components (Fig. 11), but the $KO_{II,III}$ line is recorded as a single line. The first electrons in the $P_{II,III}$-level appear for element 81 Tl, but no line resulting from the $KP_{II,III}$-transition has been detected even in 90 Th and 92 U. Obviously the line is suppressed by the neighbouring much stronger $KO_{II,III}$ line.

The intensity of the lines in the dipole doublets is proportional to the statistical weight $2J + 1$, of the doublet levels, which gives the well-known value 0.50 for the intensity ratios α_2/α_1 and β_3/β_1. It is assumed, however, that these intensity ratios could be changed for heavy elements as a result of relativistic effects, since the binding energy of the inner electrons is rather great (~ 70 keV for Au). Theoretical calculations by MASSEY and BURHOP with regard to relativistic effects show that the α_2/α_1 ratio should decrease with increasing Z. All calculations of transition probabilities in heavy atoms must necessarily include rather severe approximations, however, and MASSEY and BURHOP state that their calculations do not give a value that definitely differs from the non-relativistic value 0.50.

It is noticeable that all values for the ratio α_2/α_1 obtained in this investigation are greater than 0.50; the mean value being 0.537. VOTH reports the α_2/α_1 ratio as 0.593 and KLIEVER's Pt value is 0.52, which he states to be more reliable than the W value 0.47. It seems therefore to have been established that the α_2/α_1 ratio, that is 0.50

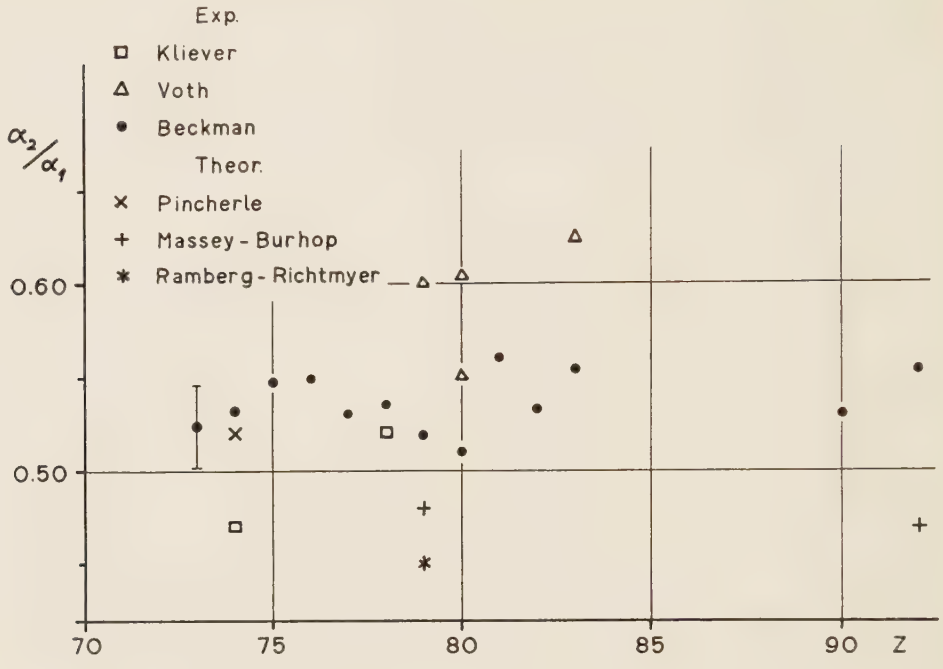

Fig. 13. The intensity ratio α_2/α_1 as a function of the atomic number Z.

for atoms in the middle of the periodic system, increases somewhat for heavy elements. The β_3/β_1 ratio obtained here (0.516) is likewise higher than 0.50, though the difference is not definitely established.

The ratios $(\beta_1 + \beta_3)/\alpha_1$ and β_2/α_1 are plotted in Figs. 14 and 15, for Z varying from 20 to 90. For elements with low Z it is impossible to resolve the β_1 and β_3 lines, and therefore MEYER's and WILLIAMS' values are compared with the $\beta_1 + \beta_3$ values obtained here for the heavy elements. WILLIAMS makes no clear distinction between transition probabilities and intensities, but since he used an ionization chamber as detector, his results are assumed to be intensity values. The values obtained by WILLIAMS and by the author are in excellent agreement in the case of $(\beta_1 + \beta_3)/\alpha_1$, but some discrepancy is shown for β_2/α_1.

The $KO_{II, III}$ line shows a rather steep increase in intensity in the Z range 73-92. An extrapolation to zero intensity for this line results in a Z value of about 65, and this would indicate that $O_{II, III}$-electrons do not appear for elements with $Z < 65$. The electrons start to enter the $O_{II, III}$-level at the element 49 In, however, and the shell is completed at 54 Xe. Further INGELSTAM [1937] reported the $KO_{II, III}$ line at 49 In and for several higher elements, so the line does exist for these elements. Obviously the $KO_{II, III}$ line intensity does not show the same steady increase with Z as do the β_1 and β_3 lines, for instance. After an initial increase for the elements just following 49 In, the line intensity then must be constant or vary only slowly until $Z \sim 72$, where the steep rise shown in Fig. 16 appears. The intensity of the line thus would show a variation with Z, similar to that of the term value r^2R of the $5p$-level (SIEGBAHN [1931] p. 389). The anomalous behaviour of the $KO_{II, III}$ line is obviously

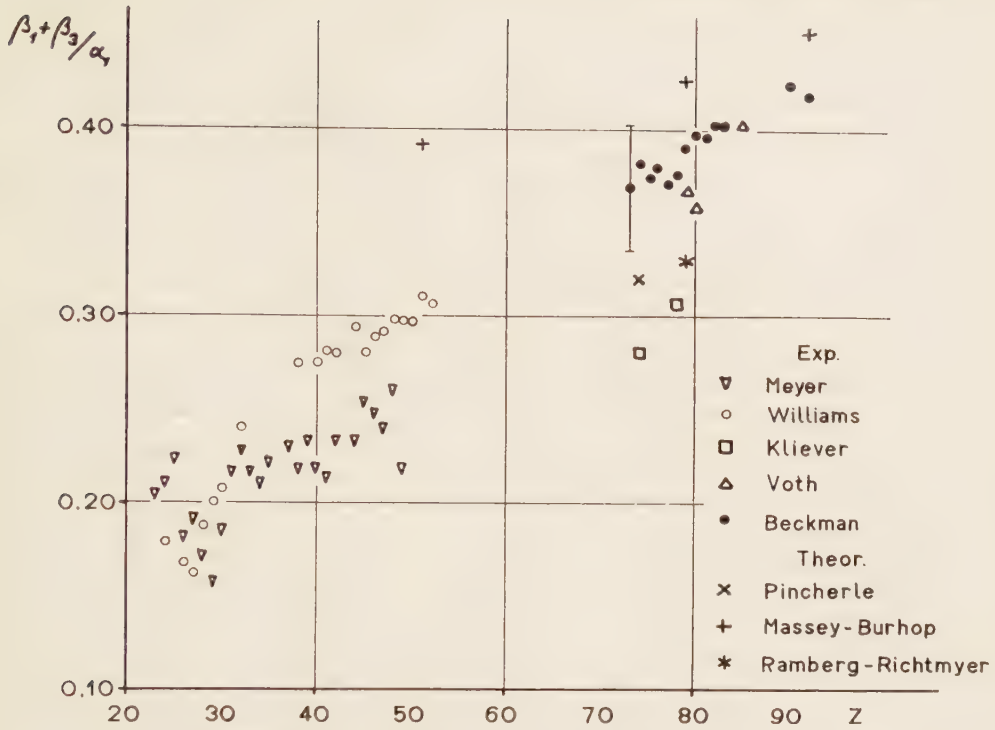

Fig. 14. The intensity ratio $(\beta_1+\beta_3)/\alpha_1$ as a function of the atomic number Z.

caused by the filling up of the 4*f*-level at the rare earth elements (Z, 58–71). The same effect, but not so pronounced, is also shown by the term value of the $N_{II,\,III}$-level and an indication of a plateau in the intensity curve for the β_2 line might explain the small discrepancy between WILLIAMS' and the author's values (Fig. 15). The same effect is reported by BRIL [1947] for the β_2 line in L-spectra (transition $L_{III}N_V$). The intensity of this line as measured relative to the $L\beta_1$ line ($L_{II}M_{IV}$) increases rapidly as Z varies from 44 to 55. In the region of the rare earths the line intensity is constant and then starts to increase slowly for $Z>72$.

b) The quadrupole lines

The two quadrupole lines, which arise from the transitions $KM_{IV,\,V}$ and $KN_{IV,\,V}$, are both doublets. The J values for the final levels are 3/2 and 5/2 respectively, which gives the theoretical intensity ratio 2:3 between the components. The β_5 line is reported separated by INGELSTAM [1937] and a slight asymmetry of the line was seen in most recordings in the present investigation too, but no attempt was made to resolve the line into its components.

The β_5/β_1 values are in general agreement with the values obtained by KLIEVER for 78 Pt and with the theoretical calculations by MASSEY and BURHOP. WILHELMY [1934] measured the β_5 and β_4 lines of 44 Ru, and reported the ratio β_5/α_1 0.0025, which fits fairly well the present values for the heavy elements. MASSEY and BURHOP have calculated the β_5/α_1 ratio at 51 Sb to be 0.0012, which shows a great discrepancy

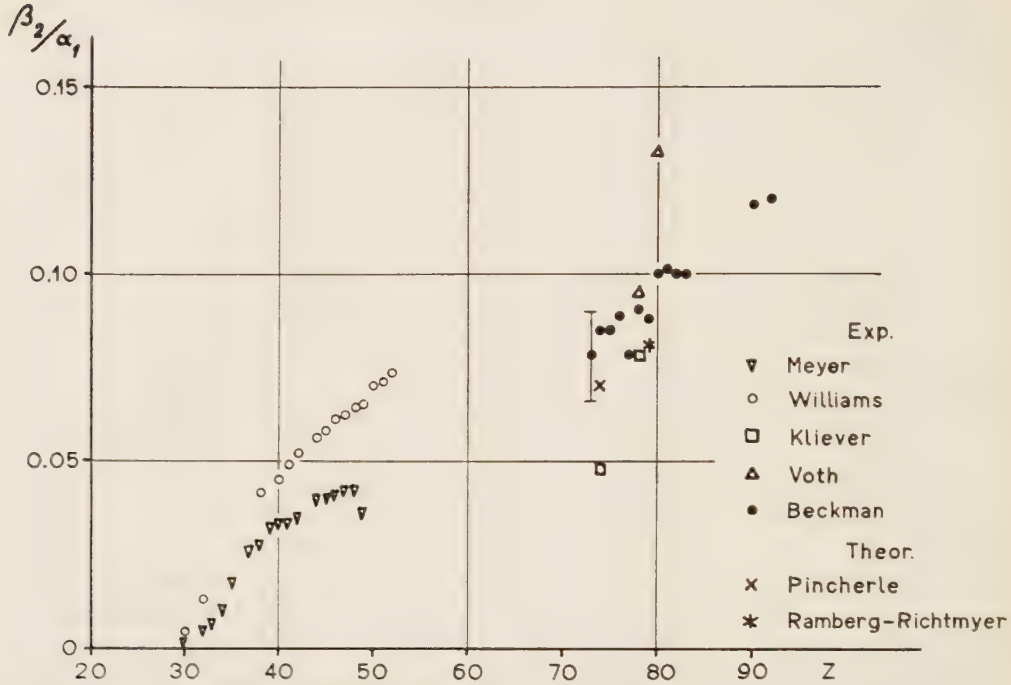

Fig. 15. The intensity ratio β_2/α_1 as a function of the atomic number Z. The values by Voth include the $KO_{II\,III}$ line.

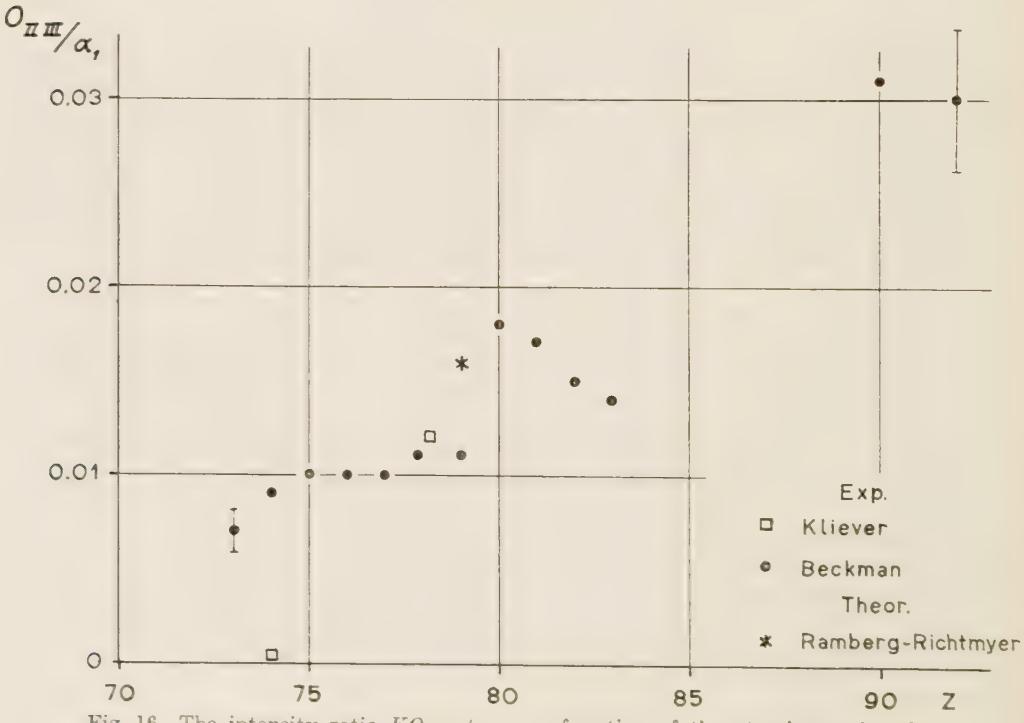

Fig. 16. The intensity ratio $KO_{II,III}/\alpha_1$ as a function of the atomic number Z.

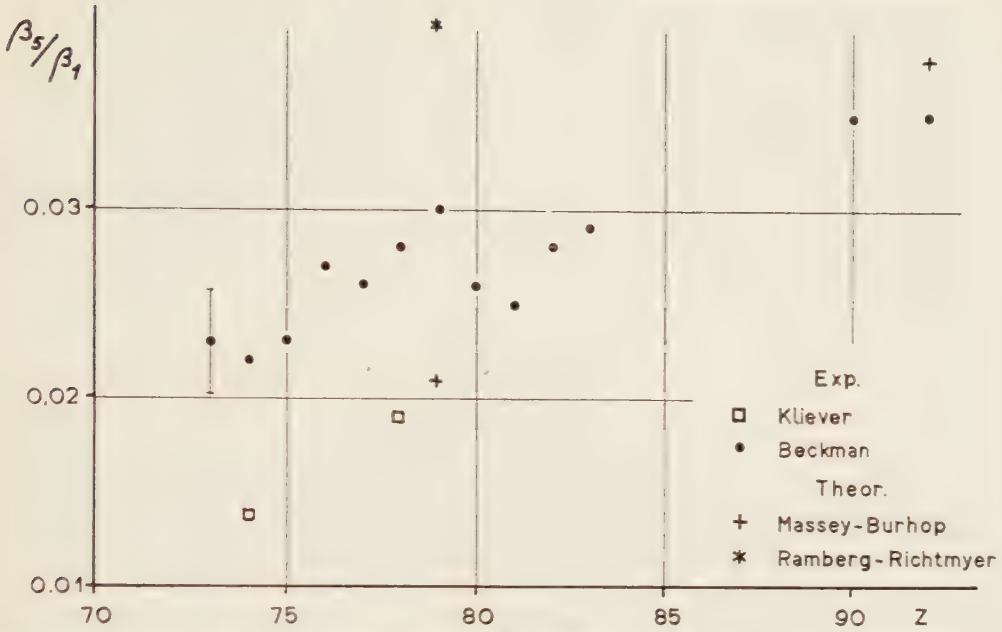

Fig. 17. The intensity of the quadrupole line β_5 compared with the intensity of the neighbouring dipole line β_1 as a function of Z.

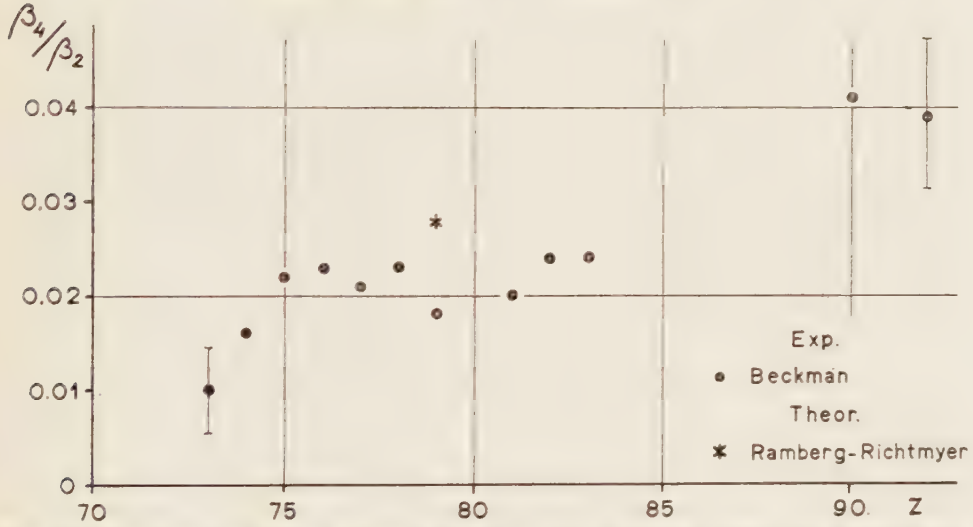

Fig. 18. The intensity of the quadrupole line β_4 compared with the intensity of the dipole line β_2 as a function of Z.

relative to WILHELMY's value. A rough calculation shows that the intensity of a quadrupole line relative to a dipole line of the same series increases as Z^2 (RUBINOWICS and BLATON [1932]). Such a Z-dependence is shown by the β_5 line: the ratio β_5/β_1 varies approximately as Z^2.

The other quadrupole line β_4 shows a much stronger Z-dependence: β_4/β_2 increases as Z^4. The β_4 line is very weak, however, and the two adjacent lines β_2 and $KO_{II,III}$ make the intensity determination very uncertain. WILHELMY reported $\beta_4/\alpha_1 = 0.006$ at 44 Ru, which seems to be in complete disagreement with the present results ($\beta_4/\alpha_1 = 0.001$ for 73 Ta). HULUBEI [1935] pointed out, however, that the β_4 line of the elements 42 Mo and 45 Rh is double and only one of the components can be referred to the $KN_{IV,V}$-transition. The other component is a non-diagram line β_{4x} (INGELSTAM [1937]). INGELSTAM followed the β_{4x} line up to the element 58 Ce; in the heavy elements this line is not detectable and only the quadrupole line β_4 is visible.

CHAPTER VI

The KL_I-transition

The K and L_I-levels are both s-levels with the total angular momentum $J = 1/2$. The KL_I line is thus forbidden both as electric dipole and quadrupole radiation. The transition can, however, occur as a magnetic dipole radiation (see p. 520). The line would thus be hard to detect but should have an intensity comparable with that of the electric quadrupole lines.

A weak line on the long wavelength side of α_2 was reported in W by DUANE and STENSTRÖM [1920] and by MAZUMDER [1927], but the identification of this line with the KL_I-transition is doubtful. More recently HULUBEI [1947] observed satellite X-ray lines on the long wavelength side of the α_2 line of several elements in the region Z, 32–42. Such satellites were also studied by GROVEN and MORLET [1951] for the elements 30 Zn and 33 As–36 Kr. The lines do not coincide in wavelength with the calculated value of the KL_I line but were assumed to be satellites of this line.

The ordinary K-satellites are caused by double-ionization of the atom. The intensity of these lines decreases roughly as Z^3 (RICHTMYER [1936]) and thus they should be extremely weak in the spectra of the higher elements. In fact they have never been observed for these elements. Instead a higher order line such as the KL_I line would probably increase in intensity with increasing Z, and since the satellites of the line

Table 10. Wavelength and intensity values of the KL_I line of 74 W and 79 Au.

Element	Wavelength XU	Intensity ($\alpha_1 = 100$)	
		Exp.	Theor. M-B.
74 W	215.33	0.14	
	53	0.22	
	54	0.12	
Mean	**215.47**	**0.16**	
79 Au	186.37	0.20	
	29	0.24	
Mean	**186.33**	**0.22**	**0.42**

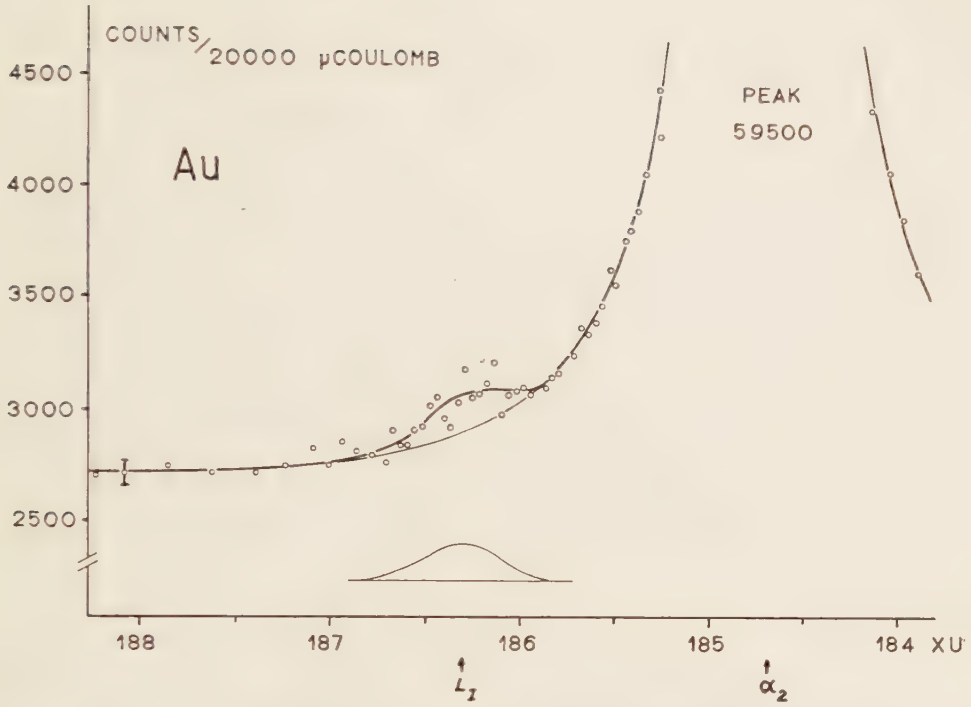

Fig. 19. The magnetic dipole line arising from the transition KL_I in gold.

are observed in the spectra of elements with low Z, the line itself might be observable in the spectra of the heaviest elements.

Special attention was thus paid to possible faint lines in the α-group of the K-spectra in the present investigation, and a very faint line was then found near the α_2 line for each of tungsten and gold, the two elements which were investigated in this respect. The wavelength values obtained for these faint lines are in agreement with the values computed from ν R data for some K and L lines of these elements. The observed line undoubtedly arises from the magnetic dipole KL_I-transition. This conclusion is supported by the work of MASSEY and BURHOP [1936] who calculated the intensity ratio of the Au KL_I line to the α_1 line to be $4.2 \cdot 10^{-3}$, which agrees moderately well with the experimental values obtained here ($2 \cdot 10^{-3}$ for Au KL_I). Table 10 contains the wavelengths and intensities obtained in the various recordings of this line in W and Au, and Fig. 19 shows one of the recordings for the Au KL_I line. The wavelength values of the lines were determined relative to the α_1 and α_2 lines, the latter wavelengths being obtained from INGELSTAM [1937]. It is further noticeable that the line is rather broad: the width of the line as obtained directly from the records is nearly double the width of the other K lines.

A transition between two levels in an atom does not necessarily give rise to an emitted X-ray quantum. The excitation energy can be transferred to an outer electron instead, with the result that this electron is ejected (Auger effect). The Auger transition probability is best known for the K-shell. For elements of low Z the Auger transition is more probable than the radiation of a quantum, but

in the heavy elements only a few per cent of the atoms excited in the K-shell emit Auger electrons (SIEGBAHN [1955]). The relative intensities of the Auger electrons have been calculated by several investigators using various electron wave functions, but the agreement with the values experimentally obtained is not good (SIEGBAHN [1955]). HILL [1953] has used another method in a calculation of the Auger intensities in the case of mercury. HILL treated the Auger effect as an internal conversion process, and assumed that the conversion coefficients for nuclear gamma-rays might be applicable to the conversion of the X-ray K-radiation in the L-subshells. This approximation would not be serious for the heavy elements where the K-shell is close to the nucleus. On account of the high conversion probability of $M1$ radiation in the L_{I}-subshell HILL was able to explain the great intensity of the Auger $KL_{\mathrm{I}}L_{\mathrm{I}}$ line assuming a probability of the KL_{I}-transition of only about 1.5 per cent of the total $E1$ X-ray radiation, which agrees with the estimation of the intensity of the satellite lines reported by GROVEN and MORLET [1951]. In the present investigation it has been found, however, that the KL_{I} line is still weaker. The intensity is only 0.2 per cent of the α_1 line, which gives too small a value of the intensity of the Auger $KL_{\mathrm{I}}L_{\mathrm{I}}$ line. The discrepancy that obviously exists may possibly be caused by the application of the gamma conversion coefficient on the X-ray K-radiation.

SUMMARY

1. A 2.5 meter focussing curved crystal X-ray spectrometer of the transmitting type is described. The spectrometer is designed for the wavelength region 100–220 XU, using the $22\bar{4}3$ plane of quartz.

2. The X-radiation has been registered by a scintillation counter with a NaI (Tl) crystal and a single channel discriminator.

3. A stabilized 800 kV van de Graaff generator was used as the high voltage source.

4. The X-ray K-spectra have been obtained for the elements 73 Ta 83 Bi, 90 Th and 92 U at 500 kV and 60–90 μA. The high luminosity of the spectrometer and the low background have made it possible to detect even the weak β_5 and β_4 lines.

5. The intensity ratios between the K lines and the $K\alpha_1$ line have been calculated. Corrections have been made for varying efficiency of the scintillation counter and for X-ray absorption within the target and in the X-ray beam between the target and the counter. The variation of reflecting properties of the crystal with the wavelength has been taken into account.

6. The theoretical calculation of the target absorption has been experimentally verified in the case of gold.

7. The calculated intensities are in general agreement with the theoretically determined values. A slight deviation from the 2 : 1 rule for the intensity ratio of some doublets is observed, however; the mean α_2/α_1 ratio is found to be 0.537 and that for β_3/β_1 is 0.516 for the elements investigated. See Table 9 and Figs. 13–18.

8. A weak line resulting from the transition K to L_{I} has been detected in the spectrum of tungsten and gold. The wavelength is: W KL_{I} 215.47 $\pm$ 0.08 XU and Au KL_{I} 186.33 $\pm$ 0.08 XU. The intensity in each case is 0.2 : 100 relative to that of the α_1 line.

REFERENCES

ÅSTRÖM, B., Arkiv f. Fysik *7*, 241 (1954).
AXEL, P., Rev. Sci. Inst. *25*, 391 (1954).
BECKMAN, O., Arkiv f. Fysik *1*, 329 (1949).
BRIL, A., Physica *13*, 481 (1947).
BROGREN, G., Arkiv f. Fysik *3*, 515 (1951).
COMPTON, A. H. and ALLISON, S. K., X-rays in Theory and Experiment, London 1935.
DUANE, W. and STENSTRÖM, W., Proc. National Acad. *6*, 477 (1920).
ELMOR, W. and SANDS, M., Electronics Experimental Techniques. New York 1949.
GOODMAN, C., The Science and Engineering of Nuclear Power. Cambridge U.S.A. 1947.
GROVEN, L. and MORLET, J., Bull. Acad. Roy. Belge Cl. Sci. *37*, 630 (1951).
HILL, R. D., Phys. Rev. *91*, 770 (1953).
HULUBEI, H., C. R. Acad. Sci. Paris *201*, 1356 (1935).
—— C. R. Acad. Sci. Paris *224*, 770 (1947).
INGELSTAM, E., Die *K*-Spektren der Schweren Elemente, Diss. Uppsala 1937.
KLIEVER, W. H., Phys. Rev. *56*, 387 (1939).
LIDÉN, K. and STARFELT, N., Arkiv f. Fysik *7*, 427 (1954).
LIND, D. A., WEST, W. J., and DUMOND, J. W. M., Phys. Rev. *77*, 475 (1950).
MASSEY, H. S. W. and BURHOP, E. H. S., Proc. Cambr. Phil. Soc. *32*, 461 (1936).
MAZUMDER, K. C., Zs. f. Phys. *46*, 449 (1927).
MEYER, H.-T., Wissenschaftliche Veröffentlichungen aus dem Siemens-Konzern *7*, 108 (1929) (ref. SIEGBAHN 1931).
MEYERHOF, W. E. and WEST, H. I., Rev. Sci. Inst. *25*, 1025 (1954).
OHLIN, P. and BECKMAN, O., Arkiv f. Fysik *1*, 323 (1949).
PINCHERLE, L., Accad. Lincei. Atti *17*, 560 (1933).
RAMBERG, E. G. and RICHTMYER, F. K., Phys. Rev. *51*, 913 (1937).
RICHTMYER, R. D., Phys. Rev. *49*, 1 (1936).
RUBINOWICZ, A. and BLATON, J., Ergebn. d. exakt. Naturwiss. *11*, 176 (1932).
SIEGBAHN, K., Beta- and Gamma-Ray Spectroscopy, Amsterdam 1955.
SIEGBAHN, M., Spektroskopie der Röntgenstrahlen, Berlin 1931.
VICTOREEN, J. A., Journ. of Appl. Phys. *20*, 1141 (1949).
VOTH, G., Ann. der Physik, *41*, 375 (1942).
WEBSTER, D. L., HANSEN, W. W., and DUVENECK, F. B., Phys. Rev. *42*, 141 (1932).
WILHELMY, E., Phys. Rev., *46*, 130 (1934).
WILLIAMS, J. H., Phys. Rev. *44*, 146 (1933).

Tryckt den 28 april 1955

Uppsala 1955. Almqvist & Wiksells Boktryckeri AB

Arkiv för Fysik

Arkiv för Fysik, the journal of physics issued by the Royal Swedish Academy of Sciences, was first published in 1949, having earlier formed part of the former *Arkiv för Matematik, Astronomi och Fysik*. The journal aims at making the research work of Swedish physicists known to the international public. The Swedish title of the journal — and of other such periodicals published by the Academy — by no means implies that Swedish is the main language used. In fact, in the volumes published so far, all papers but one are in English, German or French: Swedish authors are of course interested in making their papers understandable to all those who are working in the same field.

To facilitate subscription, *Arkiv för Fysik* will appear, from 1954 onwards, with one volume yearly. Each volume will consist of 6 issues and contain a total of about 600 pages. For Volume 8, the subscription rate is 50:— Sw. crowns.

Requests for subscription should be addressed to

ALMQVIST & WIKSELL, Import & Export Department,
Gamla Brogatan 26, Stockholm, Sweden.